

Advanced biomaterial strategies to transplant preformed micro-tissue engineered neural networks into the brain

J P Harris^{1,2}, L A Struzyna^{1,2,3}, P L Murphy¹, D O Adewole^{1,2,3}, E Kuo^{1,2} and D K Cullen^{1,2}

¹Center for Brain Injury and Repair, Department of Neurosurgery, Perelman School of Medicine, University of Pennsylvania, Philadelphia, PA, USA

²Philadelphia Veterans Affairs Medical Center, Philadelphia, PA, USA

³Department of Bioengineering, School of Engineering and Applied Science, University of Pennsylvania, Philadelphia, PA, USA

E-mail: dkacy@mail.med.upenn.edu

Received 16 January 2015, revised 3 November 2015

Accepted for publication 10 November 2015


Published 13 January 2016



CrossMark

Abstract

Objective. Connectome disruption is a hallmark of many neurological diseases and trauma with no current strategies to restore lost long-distance axonal pathways in the brain. We are creating transplantable micro-tissue engineered neural networks (micro-TENNs), which are preformed constructs consisting of embedded neurons and long axonal tracts to integrate with the nervous system to physically reconstitute lost axonal pathways. **Approach.** We advanced micro-tissue engineering techniques to generate micro-TENNs consisting of discrete populations of mature primary cerebral cortical neurons spanned by long axonal fascicles encased in miniature hydrogel micro-columns. Further, we improved the biomaterial encasement scheme by adding a thin layer of low viscosity carboxymethylcellulose (CMC) to enable needle-less insertion and rapid softening for mechanical similarity with brain tissue. **Main results.** The engineered architecture of cortical micro-TENNs facilitated robust neuronal viability and axonal cytoarchitecture to at least 22 days *in vitro*. Micro-TENNs displayed discrete neuronal populations spanned by long axonal fasciculation throughout the core, thus mimicking the general systems-level anatomy of gray matter—white matter in the brain. Additionally, micro-columns with thin CMC-coating upon mild dehydration were able to withstand a force of 893 ± 457 mN before buckling, whereas a solid agarose cylinder of similar dimensions was predicted to withstand less than $150 \mu\text{N}$ of force. This thin CMC coating increased the stiffness by three orders of magnitude, enabling needle-less insertion into brain while significantly reducing the footprint of previous needle-based delivery methods to minimize insertion trauma. **Significance.** Our novel micro-TENNs are the first strategy designed for minimally invasive implantation to facilitate nervous system repair by simultaneously providing neuronal replacement and physical reconstruction of long-distance axon pathways in the brain. The micro-TENN approach may offer the ability to treat several disorders that disrupt the connectome, including Parkinson's disease, traumatic brain injury, stroke, and brain tumor excision.

 Online supplementary data available from stacks.iop.org/JNE/13/016019/mmedia

Keywords: neurotransplantation, transplantation, bioengineering, cell replacement, axonal tracts, tissue engineering, biomaterials

(Some figures may appear in colour only in the online journal)

1. Introduction

Advances in neuroscience continue to redefine our understanding of the complexity and abilities of the brain. Due to its intricate structure as well as its robust adaptive plasticity, the human brain possesses tremendous cognitive, sensory, and motor capabilities; however, despite all of these features, the brain is rather limited to repair itself in response to a large deficit such as stroke, severe traumatic brain injury (TBI), or chronic neurodegeneration. Reasons for this include diminished intrinsic regenerative ability of neurons and the general inhibitory environment in the adult central nervous system (CNS) (Silver and Miller 2004, He 2010). Therefore, we are developing technologies to restore neural circuits in cases of long-distance deficits affecting white matter pathways in the brain (Cullen *et al* 2012, Struzyna *et al* 2015a, 2015b). In particular, we are pioneering the development of micro-tissue engineered neural networks (micro-TENNs), which are a novel class of preformed tissue engineered constructs designed for both neuronal *and* axonal tract replacement upon transplantation and functional integration with the brain. These tissue engineered 'living scaffolds' combine neural cells and biomaterials to create constructs with a defined three-dimensional (3D) axonal cytoarchitecture that can be used to (a) facilitate regeneration, (b) directly replace, and/or (c) modulate neural circuits to restore nervous system function, as well as potentially serving as (d) anatomically biofidelic models of brain micro-circuitry (Hopkins *et al* 2014, Struzyna *et al* 2015a). Utilization of these novel preformed constructs offers a unique approach to repair the nervous system in diverse conditions including Parkinson's disease, stroke, TBI, brain tumor excision, and other neurological disorders.

Numerous regenerative medicine strategies have been assessed to repair the nervous system, most of which have focused on cell-based therapies. In general, these therapies are based on the hypothesis that stem cells may provide neuroprotective factors, glial support, remyelination, or even new neurons (Tate *et al* 2002, 2004, Shear *et al* 2004, Cummings *et al* 2005, Kim 2010, Orlacchio *et al* 2010). These therapies often suffer from substantial attrition and lack of control of differentiation upon transplantation. Although these issues are actively being addressed, cell-replacement strategies alone possess an inability to guide axons to their desired end target. Several have focused on encouraging neurons to grow and regenerate axons (Jain *et al* 2004, Liu *et al* 2010, Yip *et al* 2010) whereas others have focused on creating permissive environments for axonal outgrowth (Stichel *et al* 1999, Bradbury *et al* 2002, Mingorance *et al* 2006, Tang *et al* 2007). However, these techniques do not ensure axonal outgrowth proceeds to the correct target(s) as they generally lack the specificity needed for precise reconnection and repair of long distance pathways. Recently, researchers have implanted genetically modified cells expressing developmental transcription factors to emulate development and increase targeted innervation (Grealish *et al* 2014). While these methods increased directionality, the lack of target specificity and sub-

centimeter regrowth remains insufficient for what would be required in the human brain (e.g. substantia nigra to striatum pathway is ~ 3 cm Sudheimer *et al* 2014). Thus, other strategies have attempted to enhance axonal regrowth (via biomaterials or cellular scaffolds) (Borisoff *et al* 2003, Tsai *et al* 2004, Moore *et al* 2006, Filous *et al* 2010, Silva *et al* 2010), but these methods do not replace the loss of neurons that is prevalent in neurological conditions such as Parkinson's or Alzheimer's disease. Thus, although many neurological conditions present both neuronal and axonal loss (Coleman and Perry, 2002, Bjartmar *et al* 2003, Dauer and Przedborski 2003), cell replacement strategies alone are often ill equipped to restore long distance connections, while axonal guidance techniques generally fail to address degeneration of neuronal populations.

We have advanced micro-tissue engineering techniques to create tubular biomaterial micro-columns (less than half the diameter of a DBS lead) that allow for a well-controlled 3D environment with appropriate structural and chemical cues to support neuronal survival and their long distance axonal outgrowths *in vitro*. Our concept for nervous system repair involves the implantation of preformed micro-TENNs to physically reconstruct long axonal tracts while restoring neuronal populations, relying only on local plasticity for synaptic integration to form a new functional relay across damaged connections (figure 1). As highlighted in a recent review article, there are several other methods to develop neuronal and axonal constructs, but most are focused on creating biofidelic *in vitro* models of the brain rather than replacement of neurons and their long axonal tracts in a directed manner (Hopkins *et al* 2014). Researchers have also created *in vitro* test beds where disks or cubes of neural tissue can be grown or constructed in a 3D topology, in some cases to recreate layers or self-laminating structures in biomaterial scaffolds (Cullen *et al* 2007b, Irons *et al* 2008, Dubois-Dauphin *et al* 2010, Cullen *et al* 2011, Kato-Negishi *et al* 2013, Lancaster *et al* 2013, Tang-Schomer *et al* 2014). Regardless, these efforts do not recreate the conformation of discrete neuronal populations and their lost axonal projections to distant targets. Therefore, our novel micro-TENN technology is uniquely positioned to address these capability gaps by providing a potential mechanism for neuronal replacement and precise reconstruction of axonal tracts.

In recent work, we have demonstrated initial efforts to create micro-TENNs using multiple neuronal subtypes, the ability to stereotactically deliver preformed micro-TENNs into the rodent brain, as well as transplant neuronal survival, maintenance of axonal architecture, and synaptic integration with host cortex (Struzyna *et al* 2015b). However, these previous implants required that the micro-TENN be drawn into a needle *en masse* for micro-injection, which will inherently be more damaging upon delivery than a needle-less based implant. Therefore, the current study describes improved micro-tissue engineering techniques and biomaterial encasement to allow for the needle-less insertion of fully formed, mature cortical neuronal micro-TENNs. In particular, we examined different factors associated with the *in vitro* optimization of neuronal health, neurite outgrowth, axonal

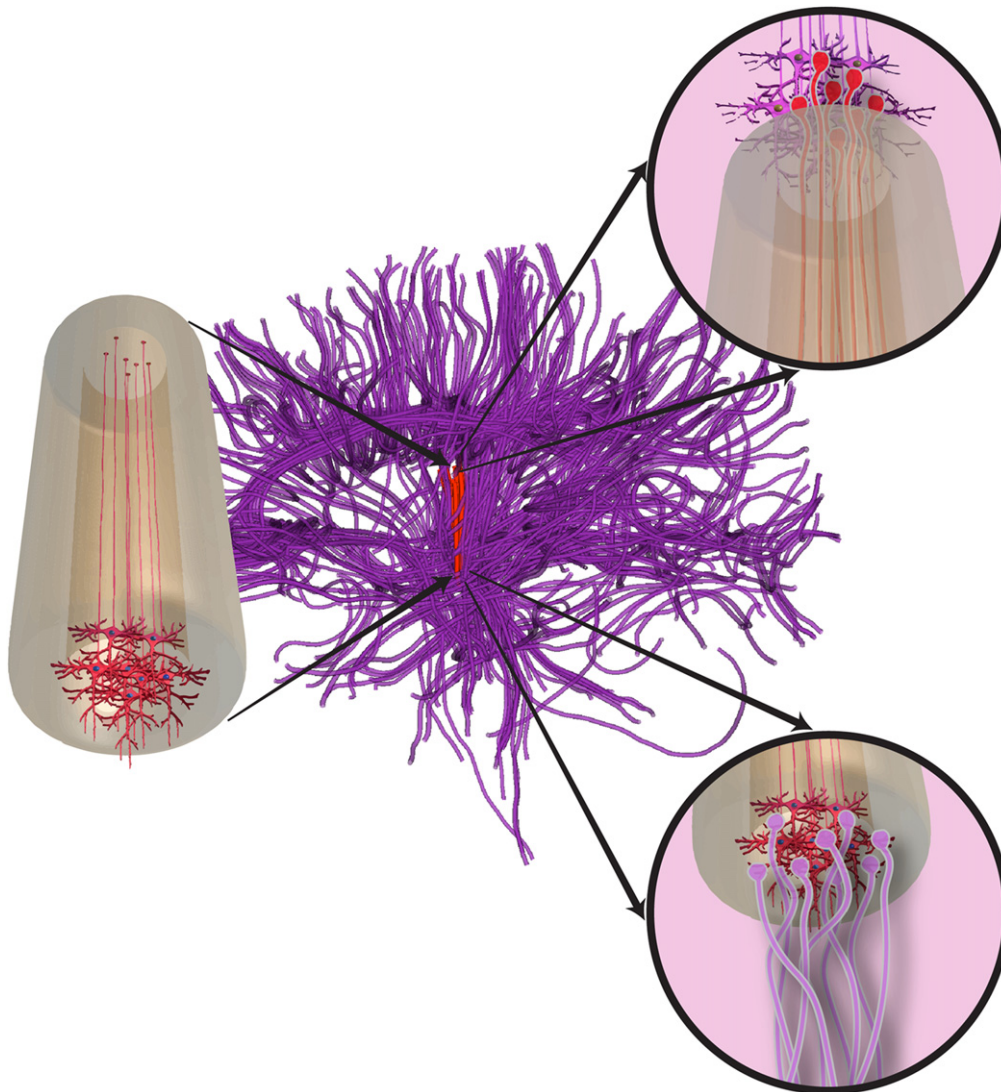


Figure 1. The micro-TENN concept. Conceptual schematic of micro-tissue engineered neural network (micro-TENN, left) with a discrete populations of neurons at one end extending unidirectional long-distance axonal projections. Micro-TENNs can be used to repair long-distance axonal pathways, depicted in tractography recreation of prominent pathways in brain (nigrostriatal pathway in red, with native axonal tracts shown as purple). Micro-TENN constructs emulate long axonal pathways with neuronal clusters at the end(s) to allow for integration with native neurons at superficial and deep targets (right, insets). This conceptual rendition depicts a ‘unidirectional’ micro-TENN with neurons only at one end; however, we have also developed ‘bidirectional’ micro-TENNs consisting of discrete neuronal populations on both ends, potentially allowing recreation of bidirectional pathways.

architecture, and maturation within micro-TENNs—thus providing improved control over the construct structure and plasticity at the time of implant. Additionally, in an effort to improve micro-TENN integration and performance *in vivo*, we have advanced an alternative micro-column construction scheme to allow for needle-less stereotaxic delivery into the brain, including a detailed examination of the mechanics required to enable needle-less insertion. An ideal needle-less insertion method will reduce the inherent micro-trauma associated with implant, thereby minimizing host reactivity and possibly improving micro-TENN survival and integration. Collectively, this work illustrates several advances in the micro-TENN technology that may ultimately enable restoration of brain circuits.

2. Materials and methods

2.1. Neural cell culture

All procedures involving animals were approved by the Institutional Animal Care and Use Committee of the University of Pennsylvania and followed the National Institutes of Health Guide for the Care and Use of Laboratory Animals (NIH Publications No. 80-23; revised 2011). Cerebral cortical neurons were isolated from Sprague-Dawley rats (Charles River, Wilmington, MA) at embryonic day 18, similar to previous work (Struzyna *et al* 2015b). Briefly, timed-pregnant rats were euthanized, and the uterus was extracted. Each fetus was removed from the amniotic sac and placed in cold HBSS. The brains were removed and the cerebral cortices were

Methods to Build Micro-TENNs

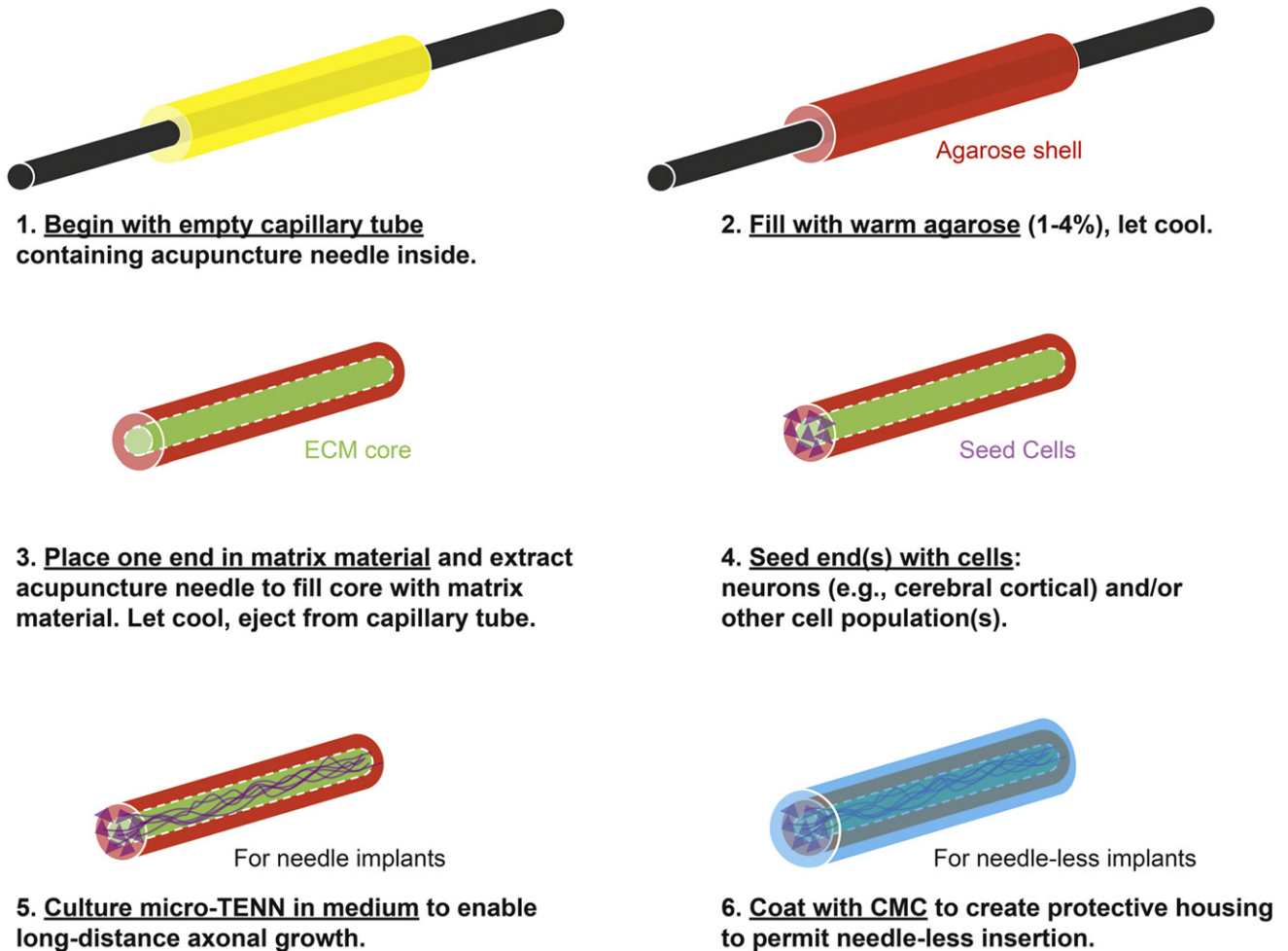


Figure 2. Overview of the micro-TENN fabrication process.

isolated via micro-dissection using a stereoscope. Cerebral cortices were placed in pre-warmed trypsin (0.25%) + EDTA (1 mM) for 12 min at 37 °C to dissociate the tissue. After removing trypsin-EDTA, the tissue was minced in HBSS containing DNase I (0.15 mg ml⁻¹). Centrifugation was performed at 1000 RPM for 3 min. Consequently, cells were resuspended at various densities (3.6, 5.6, 7.2, and 10 million cells/ml) in Neurobasal medium + 2% B27 + 0.4 mM L-glutamine (with or without a cocktail of 1 mg ml⁻¹ collagen IV + 1 mg ml⁻¹ laminin).

2.2. Micro-TENN fabrication and coating

Micro-columns consisted of a thin molded cylinder of agarose filled with extracellular matrix (ECM) through which axons could grow (see figure 2 for an overview of the fabrication process). The outer hydrogel structure consisted of 3% agarose in DPBS. The thin agarose shell was molded with an outer diameter ranging from 500 μ m to 990 μ m. To start the fabrication process, the heated agarose solution was drawn into a microliter glass capillary tube (Drummond Scientific, Broomall, PA) (figure 2(1)–(2)). An acupuncture needle

(diameter: 250 μ m–500 μ m) (Seirin, Weymouth, MA) was in the center of the liquid agarose-filled capillary tube to produce the hollow core (figure 2(1)–(2)). Once the agarose in the capillary tube had gelled (~5 min), the capillary tube was dipped into an ECM solution. The ECM solution was a collagen-laminin mixture (rat tail type I collagen, 1.0 mg ml⁻¹; mouse laminin, 1.0 mg ml⁻¹) (Reagent Proteins, San Diego, CA) solution. The needle was slowly retracted by hand at a rate slow enough to see the cloudy ECM solution climb the core. The negative pressure gradient drew the ECM solution into the hollow core (figure 2(3)). Thusly, the micro-columns featured a cylindrical agarose shell with a collagen-laminin ECM core. Micro-columns were then incubated at 37 °C for 30 min then gently ejected from the capillary tube and placed in DPBS for sterilization by UV light for 15 min.

Micro-TENNs were subsequently created by seeding micro-columns with neurons, as 10 μ l of the cell culture solution (3.6, 5.6, 7.2, and 10 million cells/ml) was delivered to both ends of the micro-columns via a micropipette while visualizing with a stereoscope (figure 2(4)). Seeded micro-TENNs were placed in a humidified tissue culture incubator (37 °C and 5% CO₂) for 75 min to allow cells to adhere.

Consequently, pre-warmed media was slowly added to the culture dish. Every 2 to 3 days *in vitro* (DIV), half media changes were performed with pre-warmed media.

For trials testing needle-less insertion, acellular micro-columns or pre-grown micro-TENNs were coated with low viscosity carboxymethylcellulose (CMC) (Sigma, C5678). All instruments were sterilized in an autoclave before preparation. In a laminar flow hood, dry CMC powder was spread evenly across a sterile glass slide using a small metal spatula to mince non-uniform particles. The CMC and all instruments utilized throughout this procedure were then illuminated with UV light for 15 min. Micro-columns were carefully extracted from media with forceps, and placed on a sterile 25G needle so that the long axis of the micro-column was parallel to the needle's long axis. The needle + micro-column was then gently rolled across in the CMC powder to coat the micro-column with a uniform layer. The micro-column was then submerged into sterile 1x PBS for approximately 3 s to hydrate the CMC coating. The micro-columns were then placed at 37 °C for dehydration, resulting in a fully encapsulated micro-column with a stiff CMC shell (figure 2(6)).

2.3. *In vitro* architecture

2.3.1. Phase imaging. *In vitro* micro-TENNs were imaged using phase-contrast on a Nikon Eclipse Ti-S microscope with digital image acquisition using a QiClick camera interfaced with Nikon Elements BR 4.10.01. To examine neuronal health and the development of axonal architecture, micro-TENNs were examined at 4–5, 7–8, 14 and 18 DIV.

2.3.2. Immunocytochemistry. Following fixation in 4% formaldehyde for 35 min, micro-TENNs were rinsed in PBS, blocked, and permeabilized with 0.3% Triton X100 plus 4% horse serum for 60 min. Primary antibody incubation was performed in PBS with 4% serum at 4 °C for 12 h. Cells were immunolabeled for: (1) MAP-2 (AB5622, 1:100, Millipore, Billerica, MA) a microtubule-associated protein expressed primarily in neuronal somata and dendrites; and (2) TUJ1/beta III Tubulin (T8578, 1:500, Sigma-Aldrich, St. Louis, MO), an element of microtubules expressed in neurites. Subsequent to rinsing, fluorescent secondary antibodies (1:500 Alexa-488, A21202, or Alexa-647, A313573, Life Technologies, Waltham, MA) were added at 18 °C–24 °C for 2 h. Finally, Hoechst (1:10 000, H3570, Life Technologies, Waltham, MA) was added at 18 °C–24 °C for 10 min. Labeled micro-TENNs were fluorescently imaged using a LSM 710 confocal microscope with a Plan-Apochromat 10x/0.45 lens (Carl Zeiss, Jena, Germany). To acquire the image, 120 slices of 2.59 μm each were acquired for each channel with 8 bit resolution. The images presented are maximum projections of the series of confocal slices.

2.3.3. Live-dead assay following CMC-coating. For live-dead analysis, micro-TENNs were coated with CMC (as described above) or left uncoated ($n = 6$ each), and were placed in pre-warmed Neurobasal media and returned to the tissue culture incubator. An additional control group was 2D neuronal

cultures grown on polystyrene ($n = 6$), which received a simultaneous media change but no CMC was added. Twenty-four hours later, micro-TENNs were rinsed with 1X PBS and incubated with 4 mM Calcein AM, 2 mM Ethidium homodimer-1 (LIVE/DEAD Viability/Cytotoxicity Kit for mammalian cells, Molecular Probes, Life Technologies, Waltham, MA) in a tissue culture incubator for 30 min. The live/dead solution was then removed, and cultures were washed three times for 10 min with 1X PBS. Samples were maintained in DPBS and imaged, as described above, within one hour of treatment with live/dead solution. The number of calcein + neurons (live) and the number of EthD-1 + nuclei (dead) were quantified across multiple regions per micro-TENN (or 2D culture) and the mean percentage of viable neurons was calculated per group.

2.4. Mechanical measurements

2.4.1. Buckling load calculations. The theoretical critical buckling force for hollow micro-columns was predicted by Euler's buckling formula (see below and Najafi and Hetke 1990). The parameter space was graphically investigated using Matlab R2014a (MathWorks, Natick, MA) by varying micro-column length, coating thickness, inner radius of coating (outer radius of agarose), and Young's Modulus of low viscosity dry CMC (Ghanbarzadeh and Almasi 2011).

2.4.2. Mechanical measurements. Mechanical testing was performed using an Instron (Norwood, MA), Model 5542, fitted with a 5 N load cell. To determine the required insertion force, stainless steel wire with a diameter approximately 508 μm (AM Systems, Part#713000) was driven into a brain phantom consisting of 0.6% agarose, which approximated the stiffness of the brain (Chen *et al* 2004). Additionally, CMC-coated micro-columns (fabricated and dehydrated as previously described) were driven into a steel plate to ascertain the critical buckling force. In order to grip the small size of the coated micro-column, a custom-machined metal collar was created to couple the load cell to a small-hole drilling adapter (McMaster-Carr, part #30505A5). Tests were done with 5 to 6 mm long micro-columns that had 3 mm protruding from the adapter holder. The Instron and control PC were programmed via Bluehill Testing software. Mechanical testing consisted of manually lowering the testing material (CMC-coated micro-column or steel wire) to identify contact with the surface, which was registered by the load cell. The implant was then backed off, and the Bluehill Testing program was activated. The program consisted of a 2 mm s⁻¹ insertion for one second based on previous reports using that insertion speed into brain (Turner *et al* 1999, Harris *et al* 2011b). Graphs of force versus displacement were used to ascertain the insertion force for steel into agarose or buckling force for CMC-coated micro-columns into a steel plate. The first peak in the graph after the artifact from the initiation of movement (Najafi and Hetke 1990, Jensen *et al* 2006, Paralikar *et al* 2006, Harris *et al* 2011b) was recorded as the insertion or buckling force.

The force from each trial was recorded, and graphed in Prism 6 (GraphPad Software, Inc., La Jolla, CA).

During buckle testing, a digital camera (Nikon D5100) filmed the insertion, buckling, and retraction movements to ensure the material under test did not move. Most images were taken using a Nikon 18–55 mm *f*/3.5–5.6G VR lens, but close up images were taken with a Tamron 90 mm *f*/2.8 SP AF Di macro lens. For the reinsertion trials, the micro-column implants remained in the brain phantom for 5–80 s before they were removed from the brain tissue and manually moved laterally to a new insertion site of agarose. The computer-controlled Instron immediately lowered the coated micro-column into the phantom at 2 mm s⁻¹.

2.5. Transplantation of micro-TENNs

Adult Sprague-Dawley rats ($n = 6$) were maintained under isoflurane anesthesia. Once anesthetized, rats were mounted in a stereotactic frame and a craniotomy was performed. Non-CMC coated or CMC-coated acellular micro-columns were drawn into a delivery needle in sterile 1X DPBS. A glass plunger was engaged within the needle inner diameter to secure the micro-column from the top. For needle injection of non-coated micro-columns ($n = 3$), the needle penetrated the brain surface to a prescribed depth, then the needle was slowly retracted while the glass plunger was in a fixed position, thus depositing the micro-columns. For the needle-less insertion of the CMC-coated micro-columns ($n = 3$), the delivery needle was placed in contact with the brain surface, and the glass plunger was engaged to gently drive the micro-column into the brain. Once micro-column delivery was complete, the craniotomy site was secured with bone wax, the scalp was sutured, and the animals were recovered. Animals were permitted to survive for 24 h post-implant for observation.

3. Results

3.1. Development of cerebral cortical neuron micro-TENN architecture *in vitro*

Previous work has illustrated that micro-TENNs derived from dorsal root ganglia can be created and survive for at least 42 DIV, and micro-TENNs derived from cerebral cortical neurons survived for at least 14 DIV (Cullen *et al* 2012, Struzyna *et al* 2015b). In the current study, our objective was to further optimize methods to generate cortical neuron micro-TENNs and allow for their maturation in culture out to at least 22 DIV, thus creating greater flexibility in neuronal maturation upon implantation. To that end, we investigated several different methods to create neuronal cultures within micro-columns. Micro-TENN neurons plated with various seeding densities demonstrated robust survival, neurite outgrowth, and various degrees of clustering (figures 3(A)–(D))—a factor necessary to produce the long axonal fascicles required to stably span long micro-column interiors. Plating densities ranging from 3.6 to 7.2 million cells/ml resulted in acute

neuronal survival and neurite outgrowth (figure 3). However, microinjection of the neurons resuspended in Neurobasal media, in contrast to a solution of collagen IV and laminin, produced a more consistent somatic clustering architecture in which discrete neuronal ganglia were connected by dense networks of neurites (figure 3). Plating at lower density, 3.6 million cells/ml, with cell delivery in Neurobasal media resulted in improved consistency in topology out to 7 to 8 DIV (figure 3(F)), with the somatic zone of the micro-column comprised of several clusters of neurons connected by dense neurite networks. Crossing the somatic zones, neurite outgrowth was seen throughout the cross section of the interior as well as at the edge of the agarose/ECM interface. Likewise, complex networks of neurites were seen throughout the micro-columns connecting multiple clusters of neurons. Notably, the combination of these factors (seeding density, dimensions, resuspension media, etc) allowed for a robust and repeatable micro-TENN topology. However, we were also able to create an alternative topology that exhibited a nucleus of neurons external to the micro-TENN channel core (figure 3(E)). This was done by having the interior ECM fill the entire tube via cutting a micro-column to the shorter length after gelation. In this fashion, when the ECM cooled and contracted, the small gaps that normally formed on the ends were removed. This topology exhibited robust neurite outgrowth exclusively into the channel core.

3.2. Architecture, length, and phenotype in mature cortical neuronal micro-TENNs

It is well established that primary neurons generally require at least 2 weeks in culture to be considered functionally ‘mature’ based on established cellular polarity, electrochemical activity (i.e., synaptic communication), inhibitory GABA currents, and expression of mature isoforms of cytoskeletal proteins (Ben-Ari *et al* 1994, Chen *et al* 1996, Steinschneider *et al* 1996, Ouardouz and Sastry 2005, Cancedda *et al* 2007, Deng *et al* 2007, Cullen *et al* 2010). Accordingly, we observed robust survival and long axonal outgrowth in micro-TENNs out to at least 22 DIV (figure 4). Indeed, over weeks micro-TENNs were shown to maintain the desired cytoarchitecture, with axons spanning over several millimeters (figure 4). Based on neuronal density and seeding parameters, micro-TENNs were created that displayed fascicular structures between neuronal clusters with long axonal ‘cables’ (figure 4(C)) or shorter intra network connections (figure 4(D)).

We found that long term neuronal survival was most consistent for micro-TENNs seeded at 3.6 million cells/ml. Here, the phenotype and structure of mature neuronal micro-TENNs was assessed at 18 DIV using immunocytochemistry and confocal microscopy (figure 5). Labeling for cell nuclei, neuronal somata/dendrites, and neurites was used to examine the different components of the neural network within the micro-column. Hoechst labeling indicated solid clusters of cells (figure 5(B)) that corresponded to cell clusters in phase image. Labeling for neuronal somata and dendrites showed correspondence with the cell clusters with local dendritic

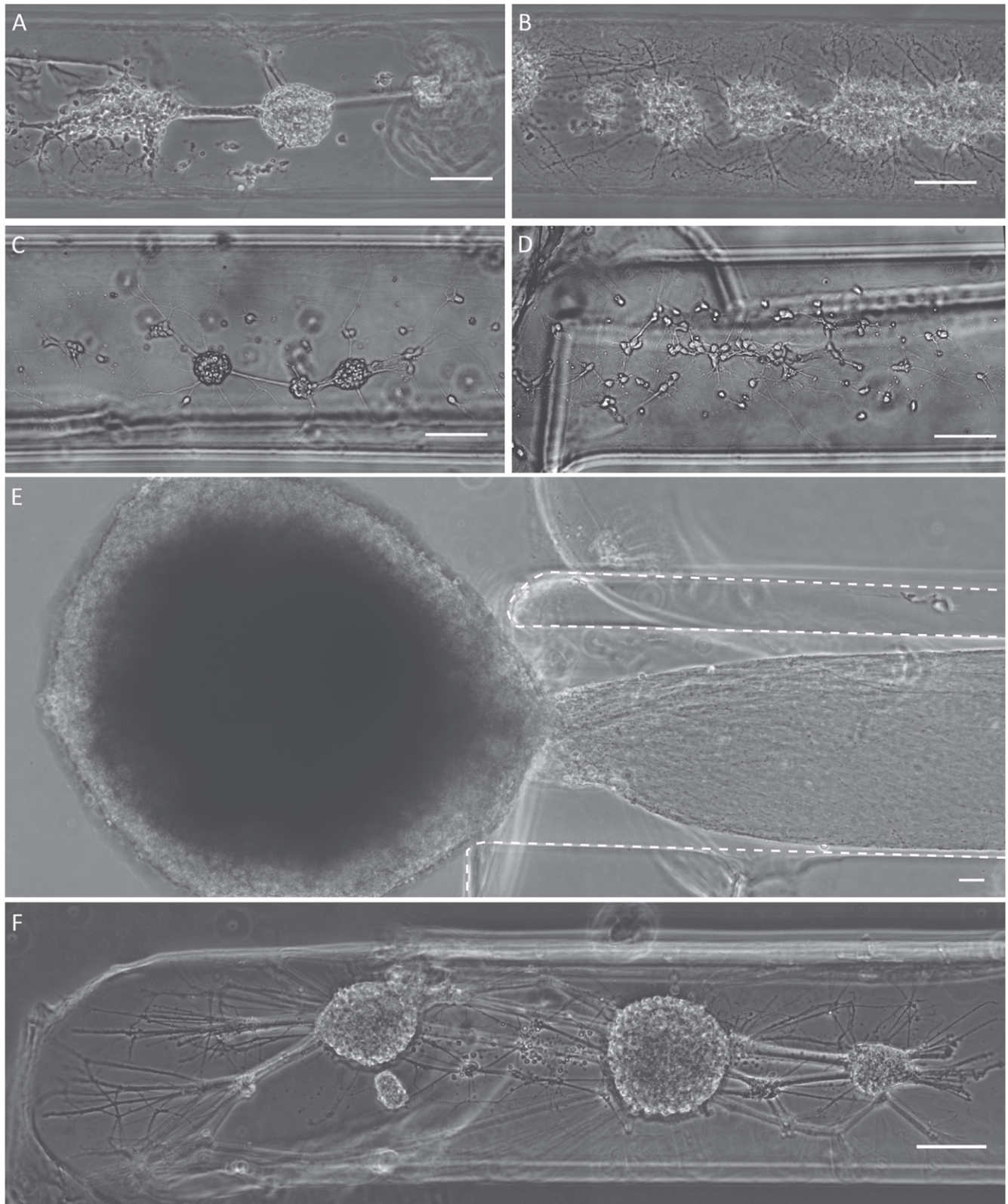


Figure 3. Micro-TENN somatic distribution based on neuronal plating and biomaterial parameters. Representative phase contrast micrographs of somatic region in immature cortical neuronal micro-TENNs at 4 to 5 DIV (A)–(D), and 7 to 8 DIV (E)–(F) plated at various neuronal densities: (A) 5.6 million cells/ml, (B), (E) 7.2 million cells/ml, (C), (D), (F) 3.6 million cells/ml. (C) Resuspending primary cortical neurons in Neurobasal media before plating produced more consistent cytoarchitecture than (D) resuspending in ECM solution (1 mg ml^{-1} collagen IV + 1 mg ml^{-1} laminin). (E) An alternative architecture was achieved where a predominant neuronal cluster remained completely external to the micro-column (dotted line = agarose walls of micro-TENN). (F) Optimal neuronal survival and cytoarchitecture at 7 to 8 DIV was achieved when neurons were plated at 3.6 million cells/ml resuspended in Neurobasal media. Scale bars = $100 \mu\text{m}$.

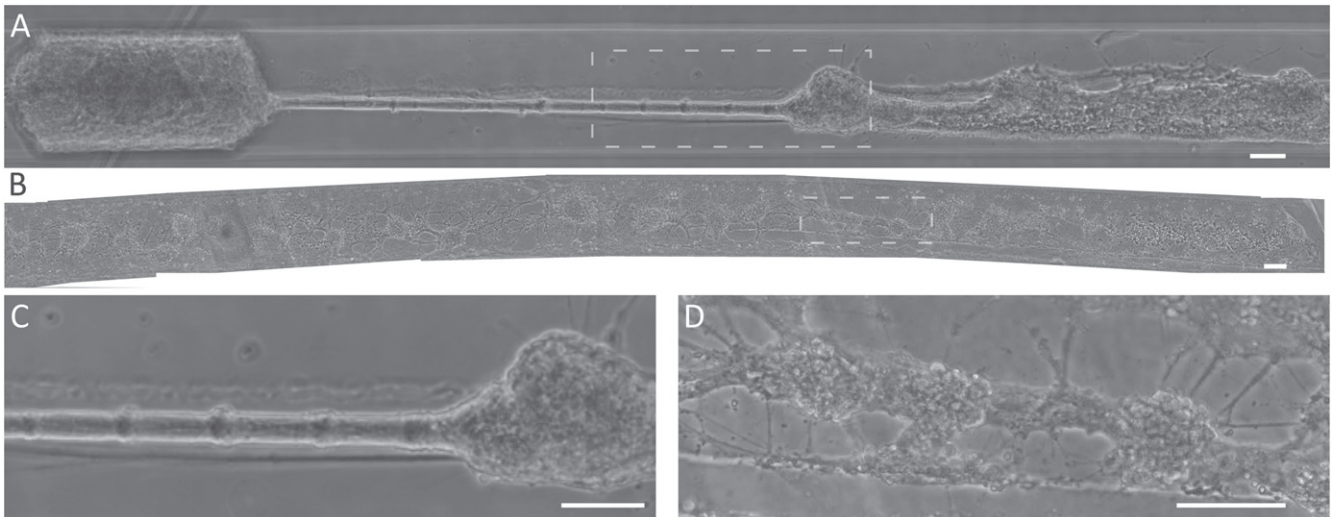


Figure 4. Neuronal and axonal cytoarchitecture in mature micro-TENNs. Representative full-length phase contrast images of mature micro-TENNs. (A) Micro-TENN at 15 DIV demonstrating dense clusters of neurons at both ends connected by ‘cable-like’ axonal fascicle, with the entire structure measuring approximately 3.7 mm in length. (B) Micro-TENN at 22 DIV exhibiting clustered neurons throughout the entire 6 mm length. (C) Enlarged region of interest from (A) showing thick axonal fascicle departing from neuronal cluster. (D) Enlarged region of interest from (B) showing neuronal clusters spanned by healthy neurite connections at 22 DIV. Scale bars = 100 μm .

networks (figure 5(C)). TUJ1 labeling (figure 5(D)) demonstrated extensive axonal outgrowth that indicated a robust and complex network of connections between neural clusters (shown as overlay in figure 5(E)). Magnification of the network indicated that cell clusters were a heterogeneous structure of somata, dendrites, and axons (figure 5(F)) while longer neurite connections consisted of robust, thick fascicles (figure 5(G); see also supplemental video S1 for confocal z-stack of 3D construct architecture). Collectively, these results demonstrate that we have advanced our neural micro-tissue engineering methodology to yield cortical neuron micro-TENNs with dense axonal fascicular connections across the micro-columns that maintained viability and health over weeks *in vitro*. This time is necessary to allow for maturation of neuronal structure and function, giving greater flexibility, engendering network stability, and potentially improving outcomes for later *in vivo* transplants.

3.3. Parameter space to enable needle-less micro-TENN insertion

Continuing upon the task to build advanced strategies to restore brain circuits via micro-TENNs, we identified the insertion method as an area for improvement. Our first design goal was to create an encasement that was stiff enough during insertion to pierce the pia of the brain without buckling. The secondary goal was for the implant to soften quickly post-insertion into the brain to better match the native mechanical properties. To satisfy these design criteria, we choose to explore the use of CMC, a common hydrogel that provides a wide range of mechanical properties based on the concentration and hydration state (Feng *et al* 2006). We used Euler’s buckling formula for a hollow cylinder to predict maximum buckling force based on Young’s modulus of dry CMC and the device dimensions (Warnock and

Benham 1965, Najafi and Hetke 1990), (equation (1a)):

$$F_{\text{crit}} = \frac{\pi^2 EI}{L_{\text{eff}}^2} \quad (1a)$$

and area moment of inertia for a hollow cylinder (equation (1b)):

$$I = \frac{\pi(r_2^4 - r_1^4)}{4}, \quad (1b)$$

where F_{crit} = the critical force when the implant buckles, I = area moment of inertia, r_2 = outer radius, r_1 = inner radius, E = Young’s Modulus of the material, L_{eff} = effective length. Approximated as a hollow cylinder, the micro-TENN was modeled with one fixed end, and one hinged end, therefore $L_{\text{eff}} = \text{Length}/\sqrt{2}$ (based on Najafi and Hetke 1990). A visual examination of the equations for a hollow cylinder and non-hollow cylinder indicated that a thin outer shell would withstand a larger buckling load than a thick inner shell. For example, a 10 μm thick shell with an $r_1 = 150 \mu\text{m}$ resulted in a term almost 150 million μm^4 greater than the inner shell term while a 10 μm shell with an $r_1 = 250 \mu\text{m}$ resulted in a term over 650 million μm^4 greater than the inner term. Therefore, we proceeded with an analysis of a thin coating (hollow cylinder) for insertion (figure 6(A)) where the maximum buckling force from Euler’s buckling equation (equation (1a)) was determined as a function of coating thickness and the outer radius of the agarose micro-column, synonymous with the inner radius of the coating. Several device lengths were examined ($L = 6, 8, 10 \text{ mm}$) with a dry CMC coating ($E = 1352.45 \text{ MPa}$) (Ghanbarzadeh and Almasi 2011). Lengths, coating thicknesses, and radii were chosen to explore a design space approximating the dimensions of constructs fabricated in this study. However, we deliberately shifted the parameter space of this theoretical

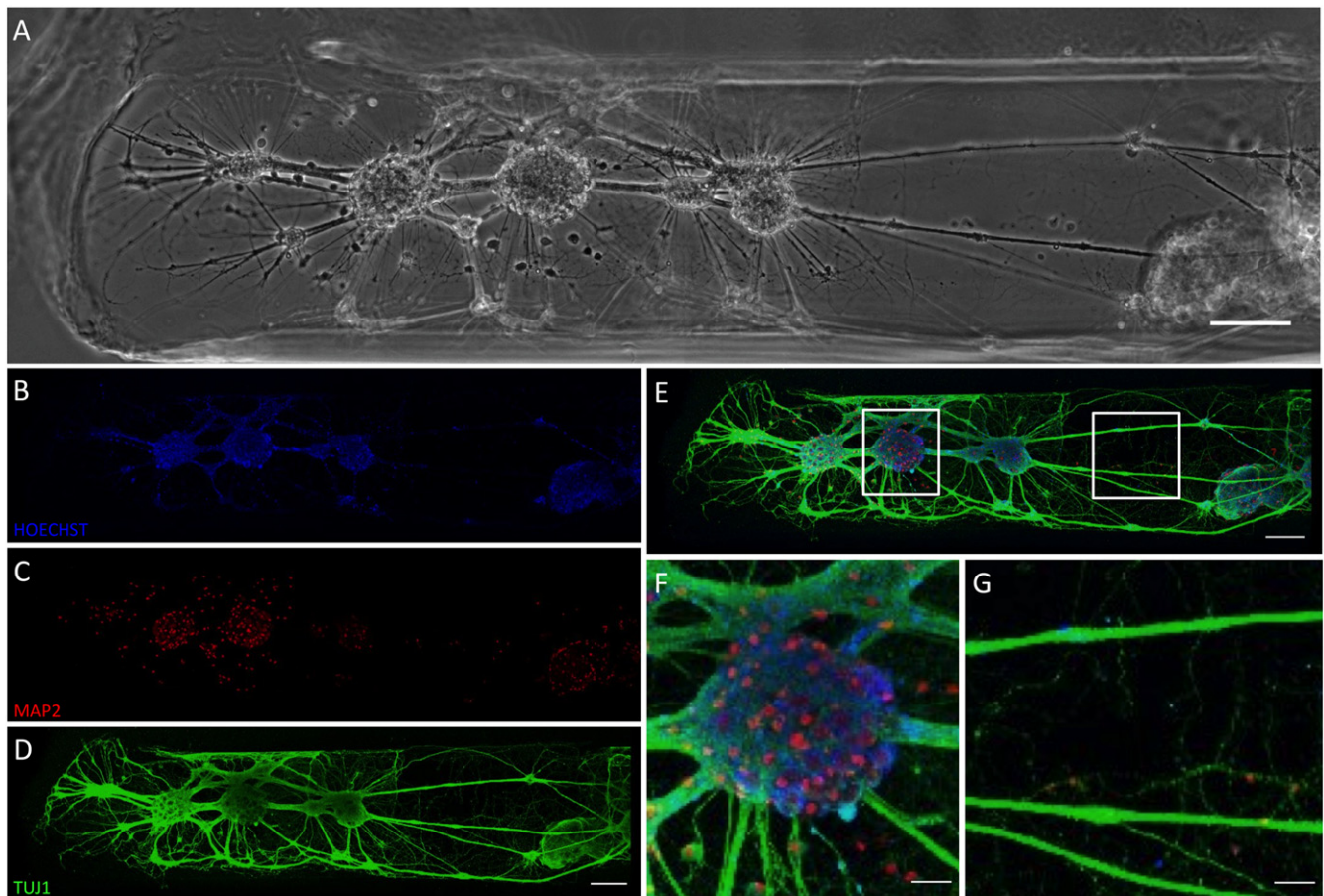


Figure 5. Neuronal phenotype and axonal structure in mature micro-TENNs. Representative mature cortical neuronal micro-TENN at 18 DIV. (A) Phase contrast micrograph showing predominant somatic region (image left, near micro-column opening) and portion of axonal region (image right, approximately mid-length). (B)–(E) Confocal 3D reconstructions of the same region shown in (A) following immunocytochemistry to label for (B) all nuclei (Hoechst, blue), (C) neuronal somata and dendrites (MAP2, red), and (D) axons (TUJ1, green), (E) with overlay. (F) Enlarged region of interest from (F) showing a representative cluster of MAP2-positive neurons projecting axonal tracts. (G) Enlarged region from (G) showing laterally projecting TUJ1-positive axonal tracts. (A)–(E) Scale bars = 100 μm . (F), (G) Scale bars = 25 μm . See supplemental video S1 for confocal z-stack demonstrating neuronal distribution and axonal growth along the contours of the micro-column inner diameter.

analysis to include longer lengths and shorter radii than those fabricated since shifting dimensions in this manner serves to lower the maximum force the micro-column can withstand, thus creating a more stringent design constraint for future device generations.

3.4. Required force for brain insertion

To ascertain whether micro-columns could theoretically be inserted directly (i.e. without a needle) into the brain, we examined the insertion force required for brain penetration. Based on literature (Chen *et al* 2004), a 0.6% agarose block was used as a phantom to simulate the stiffness and forces experienced when implanting into the brain. Initially, insertion of solid steel wire into the brain phantom was performed, revealing the peak force (occurring at approximately 1.1 mm of displacement) required to break through the surface of the agarose (figure 7(A)), akin to piercing the pia of the brain. The movement of the steel wire during the tests was illustrated by still frames (figures 7 (A1)–(A4)) and in video

(supplemental video S2), showing dimpling of the phantom surface (figure 7 (A2) and (A3)) transitioning to insertion (figure 7 (A4)). Repeated insertions of the $\sim 500 \mu\text{m}$ steel wire into 0.6% agarose yielded force graphs that were highly repeatable across multiple trials ($n = 25$). This demonstrated that the average insertion force for the implants was $22 \pm 2 \text{ mN}$ (figure 7(C), left).

3.5. Buckling and implantation forces of coated micro-TENNS

While Euler's buckling formula predicted that a thin CMC coating would enable needle-less insertion, we sought to experimentally confirm these predictions. Therefore, Instron testing was conducted on CMC-coated micro-columns to assess their maximum buckling forces. Of note, microscopic measurements revealed that CMC-coated micro-columns had a cross-section of $511.40 \pm 29.24 \mu\text{m}$. A typical Instron test showed a displacement-force graph where the force increased until a peak buckling (figure 7(B)). This behavior was illustrated by still frames (figures 7 (B1)–(B3)) showing the

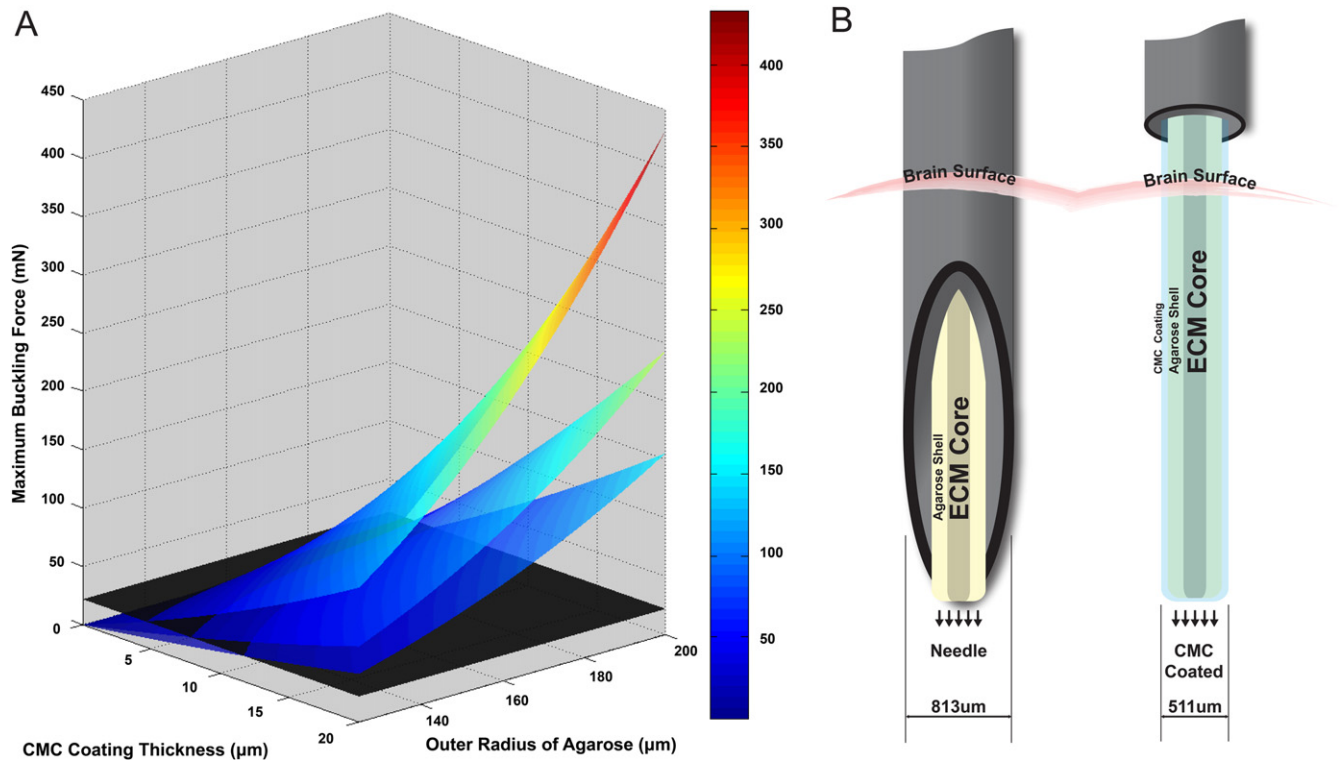


Figure 6. Biomaterial design criteria to enable needle-less implant of micro-TENNs. (A) Theoretical maximum buckling force predicted for CMC-coated micro-TENNs by Euler's buckling load formula for a hollow cylinder as a function of coating thickness, size of cylinder, and implant length (from top to bottom: 6, 8, 10 mm). The horizontal black plane represented 22 mN, the insertion force required for a $\sim 500 \mu\text{m}$ solid cylinder to be inserted into a brain phantom. The color/scale bar represents the maximum buckling force in mN. (B) Needle method ((B), left): needle and plunger system to pierce the brain surface to leave the micro-TENN in the brain parenchyma. Needle-less method ((B), right): needle lowered to surface of brain, then force applied to back end of coated micro-TENN to penetrate brain surface and ultimately rest in brain parenchyma.

CMC-coated micro-column as initially straight, but then bowing slightly and leading to buckling (also see supplemental video S3). Testing of the CMC-coated micro-column indicated that the average coated micro-column withstood a buckling force of $893 \pm 457 \text{ mN}$ ($n = 12$) (figure 7(C), right), over 40 times greater than the force required to penetrate the brain phantom (as shown above).

As a final verification, we assessed the ability of CMC-coated micro-columns to penetrate the brain phantom (our first design goal) as well as the mechanical changes in the CMC coated micro-column over time within the brain phantom, specifically the ability for CMC to quickly soften post-implant (our second design goal). This was initially tested based on insertion and reinsertion testing conducted via forceps with 1 cm long coated micro-columns. Here, coated micro-columns initially successfully penetrated the brain phantom (figure 8 (A3)), and were left in place for as little as 5 s until being removed and attempted to be reinserted into a section of the phantom lateral to the previous insertion. However, in all cases the micro-columns buckled upon reinsertion (figure 8(A5)), thus reinsertion attempts with rehydrated (i.e. softened) CMC were not successful. A similar paradigm was tested with computer-controlled insertion and reinsertion, showing that the CMC coated micro-column initially penetrated the brain phantom, but buckled immediately upon reinsertion attempt, bowing outward and

ultimately bending at a ninety-degree angle (supplemental video S4).

3.6. Insertion trajectory and *in vivo* delivery of CMC-coated acellular micro-TENNs

Another important consideration for needle-less delivery of coated micro-TENNs is the trajectory upon injection, as bending or bowing of the micro-column *in situ* would obviously affect the accuracy and consistency of stereotactic implantation. Here, a side-view of the initial insertion of CMC coated acellular micro-column demonstrated a straight, steady trajectory into the phantom brain (figures 8(B2)–(B4) and supplemental video S5), suggesting minimal additional variability in stereotactic delivery due to this methodology. In addition, as final proof-of-principle for needle-less delivery, we implanted CMC coated acellular micro-columns into the brains of anesthetized rats following craniotomy, in comparison to our standard needle injections (figures 8(C)–(F)). In all cases (3 out of 3 for each method), CMC coated micro-columns were successfully delivered into the cerebral cortices of rats. Moreover, all animals survived the procedure and recovered until the terminal time-point of 24 h with no overt adverse behavioral effects.

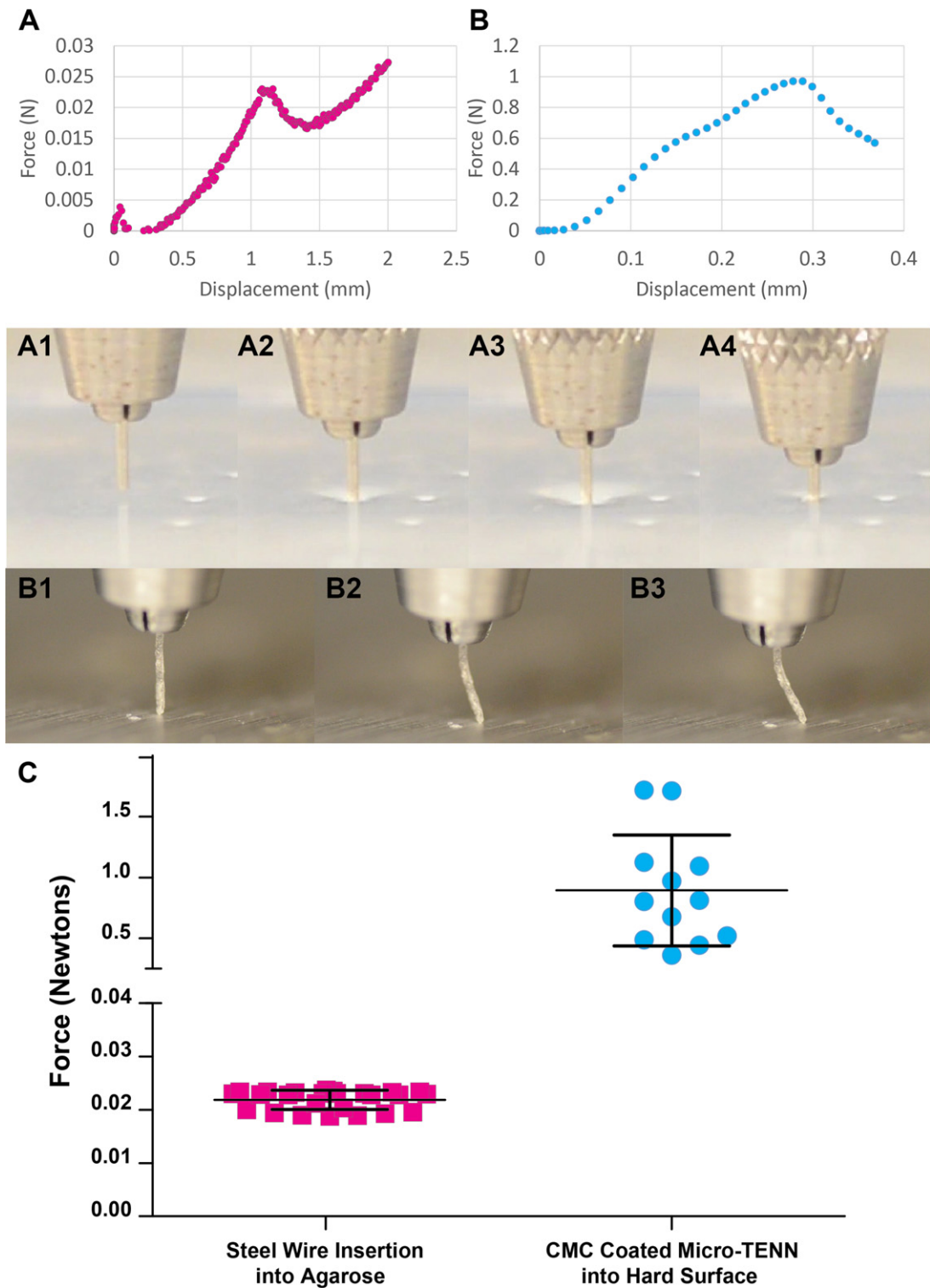


Figure 7. Mechanical testing of buckling force and phantom brain insertion force. (A) Representative trace from a stainless steel wire (diameter similar to CMC-coated micro-TENN) inserted into a 0.6% agarose (brain phantom) and (A1)–(A4) representative images of testing (also shown in supplemental video S2). The force increased as the wire was lowered into the agarose (A2)–(A3), until the agarose surface was punctured by the wire (A4). This peak at ~1.1 mm displacement was deemed the required insertion force into the brain phantom for a material of this size and shape. (B) Representative trace from CMC-coated micro-TENN that was driven into solid aluminum block, and (B1)–(B3) representative test images (also shown in supplemental video S3). The force increased until the micro-TENN buckled under the force applied (B2)–(B3), showing maximum force that the coated micro-TENN withstood before buckling (buckling force). Note (A) and (B) have different scales. (C) Graph of forces from steel wire into agarose insertion and CMC-coated micro-TENN buckling trials (error bars represent standard deviation). CMC-coated micro-TENN were able to withstand 893 ± 457 mN before buckling whereas wire required 22 ± 2 mN of force for insertion into the brain phantom, indicating that CMC-coated micro-TENN were much stronger than required for brain insertion.

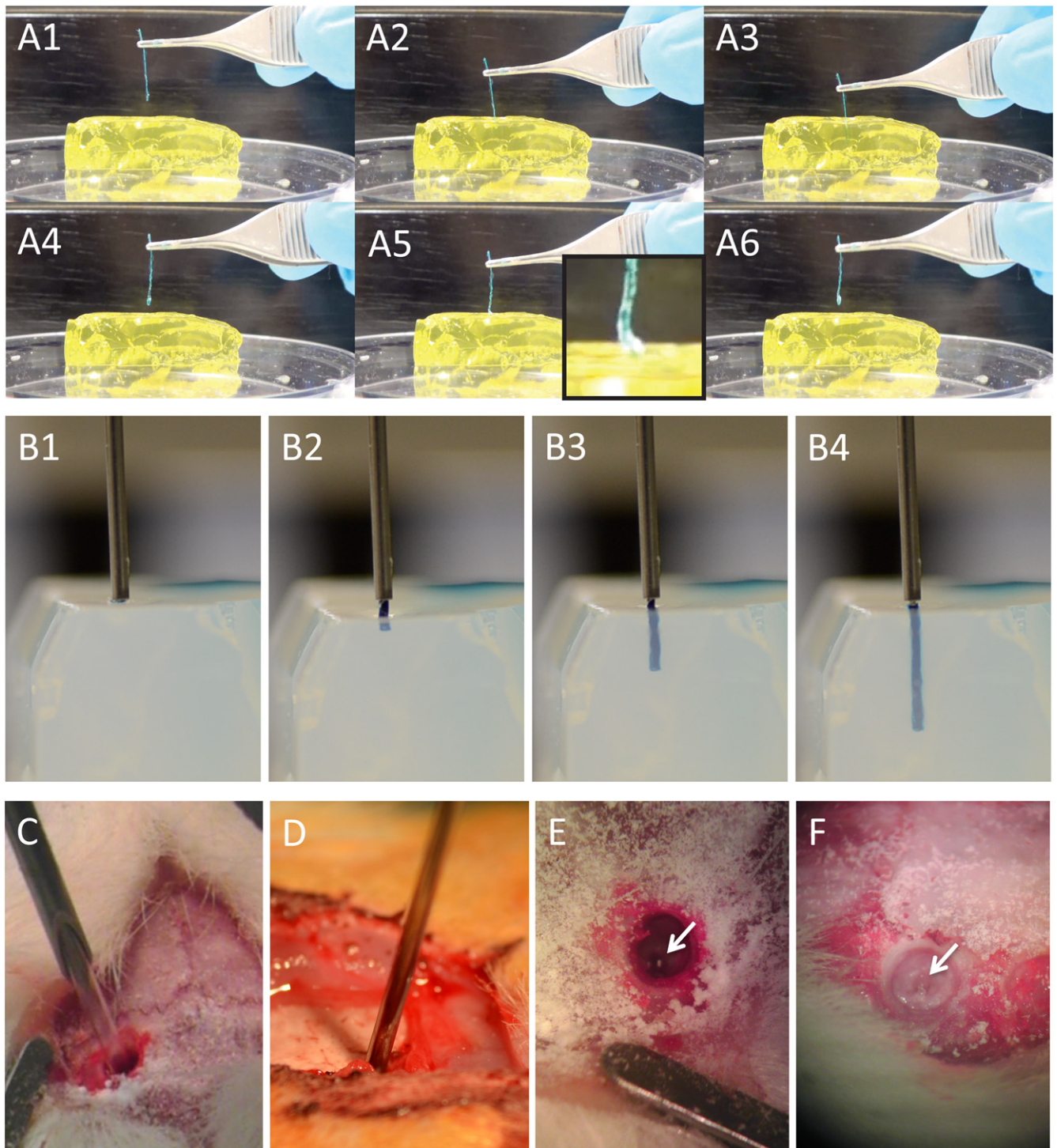


Figure 8. Needle-less insertion of CMC-coated acellular micro-columns into brain phantom and rat brain. (A1)–(A6) Video snapshots showing manual insertion of CMC-coated micro-column into brain phantom. (A1)–(A3) CMC-coated micro-column was gradually inserted into the phantom. After 5 s *in situ*, (A4) the micro-column was withdrawn. (A5) Reinsertion was attempted, but the now rehydrated CMC coating was too soft to penetrate, resulting in buckling (inset). (B1)–(B4) Video snapshots showing side view of automated insertion of CMC-coated micro-column into brain phantom. (B1) The delivery needle was lowered to the phantom surface. (B2) Force was applied to the back of the coated micro-column via a glass plunger, pushing the micro-column into the phantom. (B3) The coated micro-column followed a straight trajectory to penetrate the phantom (B4) to a depth of approximately 1 cm. (C)–(F) Stereotactic implantation of acellular micro-columns into rodent brain. (C) Needle-based injection of non-coated micro-column and (D) needle-less insertion of CMC-coated micro-column into brain. (E), (F) Examples of micro-columns *in vivo* following implantation via both methods (arrows showing proximal end just below the brain surface), confirming penetration and delivery into the brain. Note in (A) and (B) the micro-columns were dyed with blue food coloring to improve visualization before and during injection.

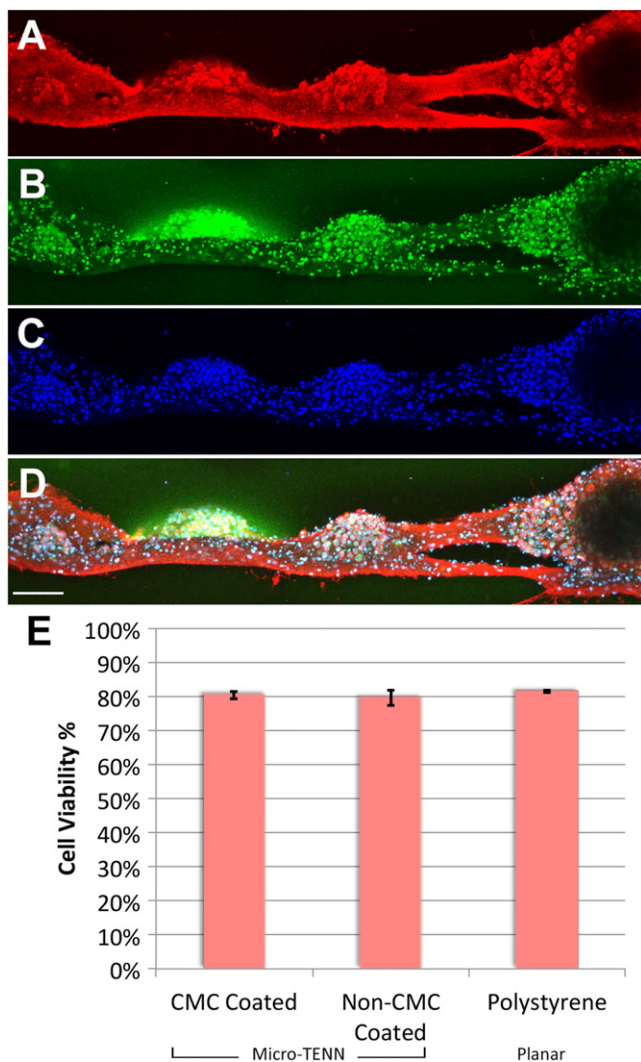


Figure 9. Cytoarchitecture and viability of CMC-coated micro-TENNs. Confocal 3D reconstructions of CMC coated micro-TENN labeled via immunocytochemistry for (A) axons (TUJ1, red), (B) neuronal dendrites and somata (MAP2, green), and (C) all nuclei (Hoechst, blue), with (D) overlay (scale bar = 100 μ m). Micro-TENN neurons and axons were healthy and intact, and appeared microstructurally identical to non-CMC coated micro-TENNs (see figure 5 for example). (E) Graph showing neuronal viability for CMC-coated micro-TENNs compared to non-coated micro-TENNs and neuronal cultures grown in 2D on polystyrene. The percentage of viable neurons was virtually identical across these groups, indicating no adverse effects of CMC coating on neuronal health within the micro-TENNs.

3.7. Effect of CMC coating on neuronal viability and cytoarchitecture

A live/dead assay was performed on neuronal networks within uncoated and coated micro-columns as well as sister 2D cultures grown on planar polystyrene dishes (absent micro-columns). This revealed that the percentage of viable neurons was $80.5 \pm 1.2\%$ for uncoated micro-TENNs, $79.6 \pm 2.2\%$ for CMC-coated micro-TENNs, and $81.5 \pm 0.2\%$ for 2D sister cultures (figure 9(E)), with no significant differences between these groups. Moreover, immunocytochemistry was performed to assess neuronal network

structure and phenotype in coated and non-coated micro-TENNs (figure 9). Immunolabeling was performed for neurites, neuronal somata and dendrites, and all nuclei, revealing that cellular structure and morphology did not vary between coated and uncoated micro-TENNs.

4. Discussion

Our novel, custom-built micro-TENNs represent a potentially transformational platform technology to model or to physically reconstruct neural circuits. The current studies represent a significant advancement in our micro-TENN strategy by improving our micro-tissue engineering and biomaterial encasement techniques. In particular, refinement of *in vitro* techniques demonstrated the ability to create cortical neuron-derived micro-TENNs exhibiting robust somatic-axonal architecture that was maintained over weeks in culture, necessary for maturation of the neuronal networks. In addition, we developed an improved biomaterial encasement strategy based on mechanical design criteria from Euler's formula, resulting in novel micro-columns that can be directly injected into brain without the need of an external needle, thus significantly reducing the footprint upon micro-TENN implantation in order to minimize surgical trauma. Although beyond the scope of the current work, the bioengineering/biomaterials advancements presented here demonstrated the feasibility of our proposed strategy, and thus enable follow-on *in vivo* studies to assess insertion damage, host responses, and micro-TENN survival and integration following needle (non-coated) versus needle-less (coated) delivery into the brain.

Our micro-TENN fabrication methodology (see figure 2) enabled control of the micro-column dimensions and the hydrogel composition. The dimensions allowed versatility in the number of neurons—and hence axons—in a given micro-TENN, with the obvious trade-off that a larger micro-TENN would result in increased brain disruption upon insertion. We previously demonstrated the creation of micro-TENNs with discrete neuronal somatic and axonal regions within 3D engineered micro-columns, with geometrical restrictions for axonal extension provided by the relatively rigid and low porosity hydrogel encasement (Cullen *et al* 2012, Struzyna *et al* 2015b). Our previous work with DRG neurons indicated that a collagen-based ECM was suitable for robust survival and long axonal extension within engineered micro-columns (Cullen *et al* 2012, Struzyna *et al* 2015b). In the case of cerebral cortical neurons, we previously found that the addition of laminin or a fibrin-based ECM was necessary to support survival and outgrowth (Struzyna *et al* 2015b). Although collagen was shown to support cortical neurons in 3D microenvironments (O'Connor *et al* 2001, Cullen *et al* 2007a), collagen alone may not have been suitable in our micro-TENNs due to the unique micro-column architecture, relatively low numbers of neurons, and extreme distances to target neurons. Moreover, in contrast to the DRG neuron-based micro-TENNs, we observed reduced clustering and increased somatic infiltration deeper into the micro-column when using cortical neurons. In our current work, we

examined several factors (e.g., cell seeding density and resuspension media) to maximize neuronal survival, clustering, and neurite outgrowth while minimizing cell infiltration. We observed that when the neurons were resuspended in Neurobasal media absent ECM constituents, more defined neuronal clusters were formed near the ends of the micro-columns. Conversely, when neurons were co-delivered within ECM (unpolymerized), we observed few neuronal clusters leading to reduced neurite outgrowth and minimal fasciculation. We believe that neuronal clustering conferred a survival advantage by increasing cell-cell interactions (e.g., trophic support) and greater regulation within the 3D microenvironment of the micro-TENNs. Conversely, the ECM cocktail further within the core of the micro-column was added before the cells were delivered, and hence was fully polymerized at the time of cell addition and therefore would not have affected neuronal re-clustering upon delivery.

An alternative successful method was to ensure that the ECM filled the entire channel (see 'alternative topology', figure 3(E)). Since the ECM contracted after it gelled in the micro-column, a micro-column that was 10% longer than desired was filled with ECM, and after gelation, the micro-column was cut to the desired length to avoid ECM voids at the ends. This 'alternative topology' is notable since the primary outer diameter of the micro-TENN could be based on axonal density and not somatic volume, and thus could be further reduced. Although not directly tested, the outer coating could then be used to encapsulate the external somatic region. Examination of the advantages/disadvantages of the alternative topology will need to be further characterized in future studies. Utilizing improved cell density/delivery and ECM protocols, we were able to produce our desired bi-directional micro-TENN cytoarchitecture: neuronal ganglia/nuclei on the micro-TENN extremities with an interior consisting predominantly of long axonal tracts (figure 4(A)).

Long-term neuronal survival within micro-TENNs is a crucial benchmark to ensure health and outgrowth of the neurons and suitability of the engineered microenvironment. This also permits control of the neuronal maturation state—likely affecting plasticity and resiliency—upon implantation into the brain. Our previous work has shown that micro-TENN viability (live/dead) or neurite morphology was not dependent on micro-TENN dimensions, but micro-TENN neurite morphology was improved with higher agarose concentrations (Struzyna *et al* 2015b). In this work, we devised methodology to create robust cortical neuronal micro-TENNs that maintained neuronal viability and the desired cytoarchitecture over several weeks *in vitro*, more similar to the longevity we previously demonstrated in DRG-based micro-TENNs *in vitro* (Struzyna *et al* 2015b). Micro-TENNs were assessed on several criteria to judge optimal health and cytoarchitecture. Healthy neurons appeared bright in phase, with full diameters and robust processes that grew thicker over time, whereas unhealthy neurons appeared dark in phase (suggestive of compaction and/or degeneration), nuclei clusters shrank over time, processes failed to extend or broke down over time, often accompanied by neurite blebbing. Applying these criteria revealed that neuronal survival within

the micro-TENNs was improved with lower cell seeding densities, consistent with cell-density dependence of neuronal survival in other 3D neural culture paradigms (LaPlaca *et al* 2010, Cullen *et al* 2011). One possible explanation for this result was that larger cell clusters could have inhibited flow of media and/or diffusion of nutrients to or waste away from neurons closer to the center of the micro-columns (Cullen *et al* 2007c, Vukasinovic *et al* 2009, Tang-Schomer *et al* 2014). Importantly, neuronal density has also been shown to directly affect the rate of neuronal maturation, synaptogenesis, and network dynamics (Wagenaar *et al* 2006, Irons *et al* 2008, Cullen *et al* 2010), and thus warrants further consideration within the micro-TENN paradigm. Phase images and immunohistochemical labeling of the micro-TENNs indicated healthy and robust mature neuronal networks (figure 5, supplemental video S1). Further characterization of neuronal phenotype, synapse formation and neurophysiology may be used in the future to more fully characterize micro-TENN structure and function.

Additionally, we advanced our biomaterial encasement strategy by adding a thin coating of CMC around the agarose micro-columns to permit needle-less delivery into brain. CMC is a common hydrogel that can be found in numerous food and biomedical products (Elliot and Ganz 1974, Bar *et al* 1995). We found that CMC coating of preformed micro-TENNs did not affect neuronal structure or viability (figure 9), consistent with a large body of literature showing that CMC and chemically-similar methylcellulose are non-toxic, biocompatible, and suitable for use in 3D neural cell culture (Bar *et al* 1995, Tate *et al* 2001, Stabenfeldt *et al* 2006, Cullen *et al* 2007b, Stabenfeldt *et al* 2010, Stabenfeldt and LaPlaca 2011, Kozai *et al* 2014). Although the CMC dehydration process need only act superficially, it is possible that this process may adversely affect the neurons within the micro-TENN core. However, the mechanics and modulus of dry CMC suggest that it is much stiffer than needed; therefore, we should be able to partially dry the coated micro-TENN to minimize the effect on neurons. Thus, the rate and time of drying may be optimized to minimize cellular effects while attaining suitable rigidity for insertion. Moreover, an additional coating to prevent moisture from leaching away from the agarose micro-column to the CMC could be devised in order to minimize hydration changes in the micro-column (and hence around the neurons) during the dehydration process. Although these studies show proof-of-principle that CMC-coated micro-TENNs can successfully be delivered into the brain, further work is required to optimize the CMC thickness and extent of dehydration to minimize swelling and host responses upon delivery, as well as to maximize transplant neuron survival—the scope for future work.

A significant advantage of our micro-TENN technology is their ability to replicate long-distance axonal connections *in vivo*. Most neural transplantation strategies for neurodegenerative disorders (Huntington's disease, Parkinson's disease, stroke, and TBI) have typically involved the transplantation of fetal grafts, single cell suspensions, or cells in 3D matrices (Fawcett *et al* 1995, Sinclair *et al* 1999, Tate

et al 2002, Tate *et al* 2009, Yoo *et al* 2011, Denham *et al* 2012, Mine *et al* 2013, Ren *et al* 2013). The delivery method for these procedures is relatively non-invasive, as it involves the injection of only a few microliters of suspended cells or an ECM hydrogel using a microsyringe (although it is noteworthy that these strategies all involve needle injection, thus the insertion trauma to host would be on par with that of micro-TENNs). These studies demonstrated varying transplant attrition rates with graft cell integration and axonal outgrowth only achieved in some cases. In contrast to our approach, recent neural cell replacement strategies have focused on the use of stem cells rather than differentiated neurons. Interestingly, recent work transplanting human embryonic stem cell neurospheres into neonatal rats demonstrated that the graft cells survived and exhibited process growth along existing white matter tracts (Denham *et al* 2012). Combinatorial approaches to deliver cells and modify the microenvironment have also been explored. For instance, a dual injection of immature astrocytes along with chondroitinase ABC reduced the presence of inhibitory ECM molecules following a micro-lesion in rats (Filous *et al* 2010). In addition, co-delivery of neural stem cells with pro-survival ECM molecules was shown to improve transplant cell survival and integration *in vivo* (Tate *et al* 2002, Stabenfeldt *et al* 2010, Stabenfeldt and LaPlaca 2011), as well as in an *in vitro* test-bed (Cullen *et al* 2007b). The co-delivery strategy of cells and ECM (presenting pro-survival ligands) is built into the ‘living scaffold’ concept employed in micro-TENNs, with the added feature that micro-TENNs possess a pre-defined cytoarchitecture. The neural cells and ECM core present molecules that may facilitate survival, outgrowth, and plasticity to facilitate incorporation into native neural networks upon delivery into the brain. While previous work provides remarkable advances and hope for eventual repair of the nervous system, micro-TENNs represent a promising strategy to simultaneously replace neural cells as well as their long-distance axonal connections.

While the advantages of micro-TENNs are appealing, the abilities of the construct would be improved given methodology for reliable delivery into the brain with minimal insertion damage. To that end, we undertook a process to design and create a needle-less insertion method. An insertion event will cause microhemorrhaging that will initiate the acute inflammatory response. Unfortunately, the potential for a trauma-less insertion is impossible since neurons are typically within 15 μm of a capillary, although separation from larger vessels is greater (Tsai *et al* 2009). Vasculature disruption results in a response to repair the damaged vessels. If the disruption cannot be resolved or the blood–brain barrier remains leaky, blood factors can continue to infiltrate the brain parenchyma leading to a chronic response. The chronic response could create an inhospitable environment causing implanted (and host) neurons to degenerate. While many implant factors are believed to play a role in the chronic response (Harris and Tyler 2014), it is generally believed that device size, stiffness, and material composition are key considerations. Other researchers have shown that implantation of a smaller device resulted in a reduction of both the acute

scarring response at three days after implant as well as the chronic response (up to 12 weeks) (Seymour and Kipke 2007, Karumbaiah *et al* 2013). Therefore, our goals for a biomaterial-based insertion method were to minimize the insertion footprint by utilizing a construct rigid enough for insertion, but ultimately having the construct soften after insertion to better match the mechanical properties of the brain.

To reach these goals, we utilized Euler’s formula to predict relevant design parameters for needle-less insertion (figure 6(A)). This analysis revealed that a thin external coating would buckle at a higher load than a thick internal core with the additional advantage that a thin coating could quickly dissolve, to leave the hydrophilic, soft hydrogel to minimize the chronic response to the implant due to implant stiffness. We found that the insertion force required for a $\sim 500 \mu\text{m}$ wire to penetrate into a brain phantom was approximately 22 mN (measurements shown in figure 7(C), left). Although 22 mN was larger than other previously published figures for insertion force into the brain of $\sim 4 \text{ mN}$ (Najafi and Hetke 1990, Harris *et al* 2011b), our implant cross section was an order of magnitude larger and without a pointed tip. Thus, we used 22 mN as the threshold force level for needle-less delivery, represented by the black plane in figure 6(A) depicting the results of our theoretical analysis of various micro-column dimensions. Here, for points on a surface that lay above the horizontal black plane, Euler’s buckling formula predicted that the micro-column would be successfully implanted into the brain without buckling—thus predicting that CMC-coated micro-columns of the dimensions used in this study would not buckle upon brain insertion. Indeed, since the thin coating of CMC provided such an increase in buckling force, we examined lengths ($L = 6, 8, 10 \text{ mm}$) much longer than would be needed for near-term rodent studies. In comparison, Euler’s formula suggested that a $500 \mu\text{m}$ solid 3% agarose tube would only be able to withstand 0.14 mN before buckling (3 mm length, 3% agarose modulus = 20 kPa Mauck *et al* 2000). While the exact dimensions of the CMC coating thickness used in our studies was not ascertained (we estimate the CMC thickness to be approximately 10 μm), the measurement of the buckling force was $893 \pm 457 \text{ mN}$ (figure 7(C), right), demonstrating that the CMC coated micro-TENN was more than sufficient to meet the insertion requirement of 22 mN. Moreover, any differences between Euler’s formula/graph and experimental data were assumed to be from CMC not being not completely dehydrated, resulting in a modulus lower than the $E = 1352.45 \text{ MPa}$ for dry CMC (Ghanbarzadeh and Almasi 2011). Fortunately, even partial drying was enough to enable insertion of the CMC-coated micro-column (figure 8 and supplemental videos S4 and S5). Additionally, the CMC-coating quickly softened, not allowing for reinsertion (figure 8 and supplemental video S4), thus demonstrating closer mechanical properties to brain. Importantly, this method resulted in coated micro-columns with mean cross-section of approximately 511 μm compared to recent needle-based micro-TENN insertions with an outer diameter of 813 μm (Struzyna *et al* 2015b). Therefore, the needle-less method had a footprint that was less than two-thirds of the

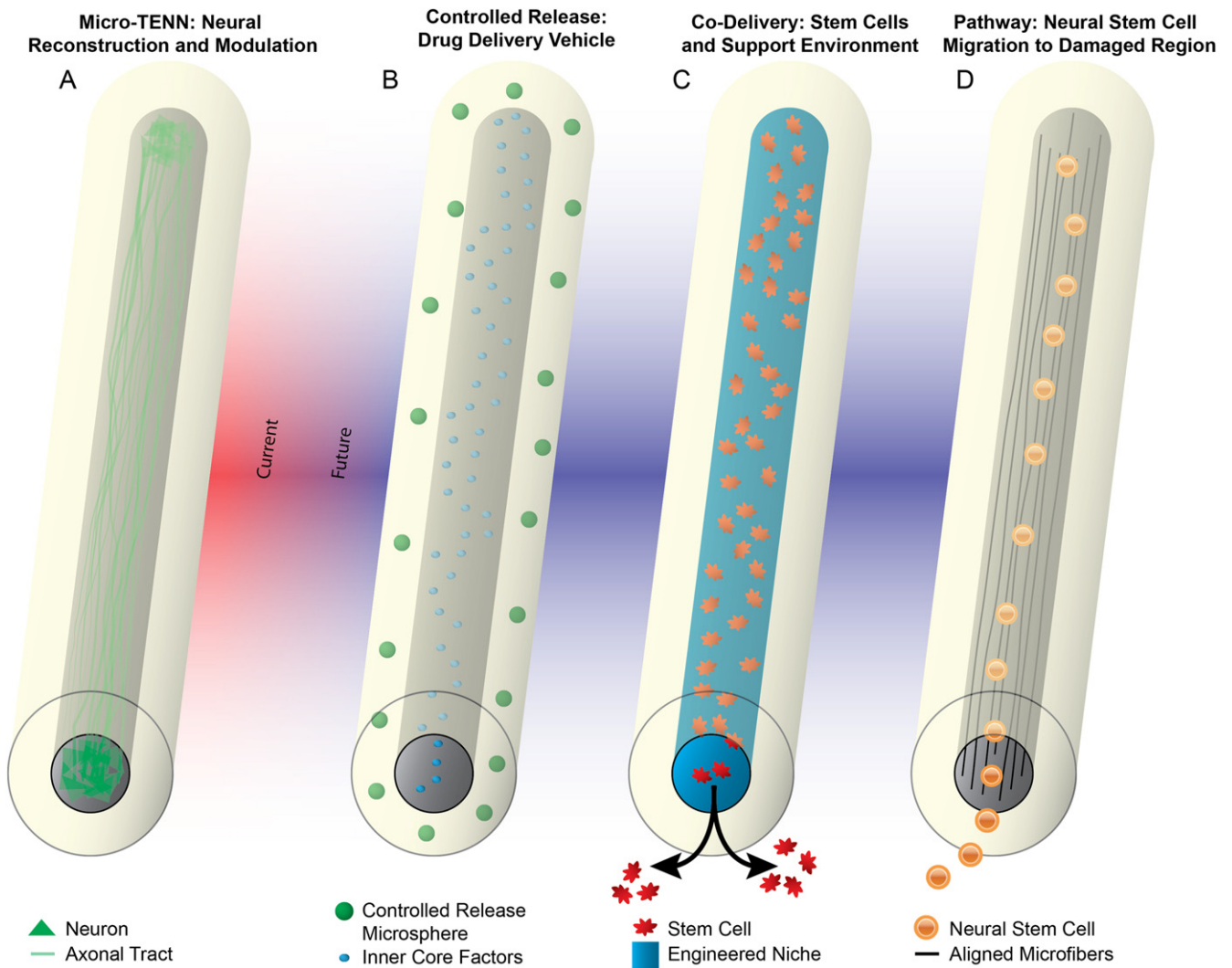


Figure 10. Future applications of the micro-column technology. Micro-columns provide a unique biological and mechanical topology consisting of a protective outer shell with a well-controlled inner core, thus enabling a myriad of other usage scenarios. (A) As established in this and previous work, preformed micro-TENNs provide a suitable medium to grow neurons with long axonal outgrowth *in vitro* that can be implanted *en masse* to serve as living scaffolds to reconstruct long-distance axonal pathways. (B) Micro-columns could also provide an alternative form factor for a long-aspect ratio controlled release construct. Utilizing the multi-layered nature of the micro-columns, the outer shell(s) and the inner core can be constructed to release different factors over different time courses and regions along a longitudinal neuroanatomical structure. (C) Leveraging the protective outer layer, micro-columns could allow for a mechanical and biological buffer from the brain microenvironment to co-deliver stem cells in a precisely engineered niche, which could control differentiation, activity, and migration *in situ*. (D) Finally, micro-columns could be fabricated to serve as migratory pathways for endogenous neural stem cells from a point of birth to a region experiencing significant degeneration. This may be accomplished using aligned microfibers and/or gradients within the core, and this protective milieu may also affect stem cell differentiation and activity.

needle method, suggesting that the needle-less method would cause significantly less insertion damage and thus may provide a more hospitable environment for implanted neurons to integrate with the native nervous system, although follow-up studies are required to experimentally test this hypothesis.

5. Conclusions and future directions

Through this work and previous work (Cullen *et al* 2012, Struzyna *et al* 2015b), we have firmly established micro-TENNs as promising constructs for direct neural reconstruction and modulation (figure 10(A)). However, we foresee

that our novel micro-column platform may be efficacious for other neuroregenerative medicine applications as well (figures 10(B)–(D)). By successfully replacing lost neuronal populations, integrating with host neural circuitry, and re-establishing lost axonal tracts, we foresee these unique micro-TENNs facilitating nervous system repair and functional recovery. Of note, although the primary purpose of the current iteration of micro-TENNs is to replace white matter pathways, this requires integration and potentially neuronal replacement in gray matter; thus, micro-TENNs are designed to affect white and gray matter. Although our early results with micro-TENN technology are promising, there are challenges to be addressed *in vitro* such as the creation of novel

types of micro-TENNs with controlled neuronal populations for improved specificity of integration *in vivo*. In addition, there are several preclinical efficacy milestones before micro-TENNs can be translated clinically, including the demonstration of micro-TENN structural connectivity, electrophysiological integration, and behavioral recovery in preclinical CNS models of injury and/or neurodegeneration. Moreover, despite the small dimensions of the micro-TENNs and the ability to deliver them in a minimally invasive fashion (based on the needle-less methodology described here), their delivery still constitutes a ‘micro-stab’ wound to the brain. As such, there will be an acute inflammatory response upon delivery that may affect micro-TENN neuronal survival and integration. While the relative softness of the agarose casing should minimize a gliotic response by minimizing mechanical mismatch with the brain (Harris *et al* 2011a, Moshayedi *et al* 2014, Nguyen *et al* 2014), even the short-term presence of a foreign hydrogel material may generate an inflammatory response. Therefore, it may be necessary in future studies to design the tubular agarose shell as a vehicle for controlled delivery of anti-inflammatory, pro-survival, and/or pro-plasticity agents in a precise spatiotemporal manner (thus combining features theorized in figure 10). Moreover, although we and others have shown that allogeneic constructs consisting of pure neurons appear to be immune-privileged in rats and pigs (Iwata *et al* 2006, Huang *et al* 2009, Liu *et al* 2012, Struzyna *et al* 2015b), chronic immune tolerance will need to be verified in future studies. However, we ultimately envision that this micro-tissue engineering approach will converge with stem cell-based methods to generate autologous micro-TENNs, thus enabling the creation of tailored constructs to mimic the precise cytoarchitecture and extent of repair necessary on a per patient basis. Moreover, the translation of micro-TENNs or similar neuroregenerative medicine technology will require the development of new neurosurgical, manufacturing, construct handling, and quality control protocols.

Overall, our novel micro-TENNs represent a promising strategy capable of simultaneously restoring lost neuronal populations and long-projecting axonal tracts following major CNS degeneration. Indeed, the current work provides a foundation to enable future *in vivo* studies to assess the efficacy of micro-TENNs to survive, functionally integrate, and restore function within the damaged CNS. With future advancement, micro-TENNs offer an attractive and unique strategy to treat a range of neurological disorders, including Parkinson’s disease, TBI, stroke, and other neurodegenerative diseases.

Acknowledgments

Financial support was provided by the Penn Medicine Neuroscience Center, National Science Foundation (Graduate Research Fellowship DGE-1321851), National Institutes of Health (T32-NS043126 & T32-GM007517), Department of Veterans Affairs (RR&D Merit Review #B1097-I), and the US Army Medical Research and Materiel Command through

the Joint Warfighter Medical Research Program (#W81XWH-13-207 004). The authors would like to thank Rob Mauck and Mike Hast in the Penn Center for Musculoskeletal Disorders Core for help in mechanical testing. Additional thanks go to Vincent Wu, Norma Alexis Brown, Alan He, Camila Robles-Oteiza, and Parker Schabel for technical contributions.

References

- Bär A, Til H P and Timonen M 1995 Subchronic oral toxicity study with regular and enzymatically depolymerized sodium carboxymethylcellulose in rats *Food. Chem. Toxicol.* **33** 909–17 (PMID: 7590537)
- Ben-Ari Y, Tseeb V, Ragozzino D, Khazipov R and Gaiarsa J L 1994 Gamma-Aminobutyric acid (GABA): a fast excitatory transmitter which may regulate the development of hippocampal neurones in early postnatal life *Prog. Brain Res.* **102** 261–73
- Bjartmar C, Wujek J and Trapp B 2003 Axonal loss in the pathology of MS: consequences for understanding the progressive phase of the disease *J. Neurological Sci.* **206** 165–71
- Borisoff J F, Chan C C, Hiebert G W, Oschipok L, Robertson G S, Zamboni R, Steeves J D and Tetzlaff W 2003 Suppression of Rho-kinase activity promotes axonal growth on inhibitory CNS substrates *Mol. Cell. Neurosci.* **22** 405–16
- Bradbury E J, Moon L D, Popat R J, King V R, Bennett G S, Patel P N, Fawcett J W and McMahon S B 2002 Chondroitinase ABC promotes functional recovery after spinal cord injury *Nature* **416** 636–40
- Cancedda L, Fiumelli H, Chen K and Poo M M 2007 Excitatory GABA action is essential for morphological maturation of cortical neurons *in vivo* *J. Neurosci.* **27** 5224–35
- Chen G, Trombley P Q and van den Pol A N 1996 Excitatory actions of GABA in developing rat hypothalamic neurones *J. Physiol.* **494** 451–64
- Chen Z-J, Gillies G T, Broaddus W C, Prabhu S S, Fillmore H, Mitchell R M, Corwin F D and Fatouros P P 2004 A realistic brain tissue phantom for intraparenchymal infusion studies *J. Neurosurgery* **101** 314–22
- Coleman M P and Perry V H 2002 Axon pathology in neurological disease: a neglected therapeutic target *Trends Neurosci.* **25** 532–7
- Cullen D K, Gilroy M E, Irons H R and Laplaca M C 2010 Synapse-to-neuron ratio is inversely related to neuronal density in mature neuronal cultures *Brain Res.* **1359** 44–55
- Cullen D K, Lessing M C and LaPlaca M C 2007a Collagen-dependent neurite outgrowth and response to dynamic deformation in three-dimensional neuronal cultures *Ann. Biomed. Eng.* **35** 835–46
- Cullen D K, Stabenfeldt S E, Simon C M, Tate C C and LaPlaca M C 2007b *In vitro* neural injury model for optimization of tissue-engineered constructs *J. Neurosci. Res.* **85** 3642–51
- Cullen D K, Vukasinovic J, Glezer A and LaPlaca M C 2007c Microfluidic engineered high cell density three-dimensional neural cultures *J. Neural Eng.* **4** 159
- Cullen D K, Tang-Schomer M D, Struzyna L A, Patel A R, Johnson V E, Wolf J A and Smith D H 2012 Microtissue engineered constructs with living axons for targeted nervous system reconstruction *Tissue Eng. A* **18** 2280–9
- Cullen D K, Wolf J A, Vernekar V N, Vukasinovic J and LaPlaca M C 2011 Neural tissue engineering and biohybridized microsystems for neurobiological investigation *in vitro* (part 1) *Crit. Rev. Biomed. Eng.* **39** 201–40

- Cummings B J, Uchida N, Tamaki S J, Salazar D L, Hooshmand M, Summers R, Gage F H and Anderson A J 2005 Human neural stem cells differentiate and promote locomotor recovery in spinal cord-injured mice *Proc. Natl Acad. Sci. USA* **102** 14069–74
- Dauer W and Przedborski S 2003 Parkinson's disease: mechanisms and models *Neuron* **39** 889–909
- Deng L, Yao J, Fang C, Dong N, Luscher B and Chen G 2007 Sequential postsynaptic maturation governs the temporal order of GABAergic and glutamatergic synaptogenesis in rat embryonic cultures *J. Neurosci.* **27** 10860–9
- Denham M, Parish C L, Leaw B, Wright J, Reid C A, Petrou S, Dottori M and Thompson L H 2012 Neurons derived from human embryonic stem cells extend long-distance axonal projections through growth along host white matter tracts after intra-cerebral transplantation *Front. Cell Neurosci.* **6** 11
- Dubois-Dauphin M L, Toni N, Julien S D, Charvet I, Sundstrom L E and Stoppini L 2010 The long-term survival of *in vitro* engineered nervous tissue derived from the specific neural differentiation of mouse embryonic stem cells *Biomaterials* **31** 7032–42
- Elliot J H and Ganz A 1974 Some rheological properties of sodium carboxymethylcellulose solutions and gels *Rheol. Acta* **13** 670–4
- Fawcett J W, Barker R A and Dunnett S B 1995 Dopaminergic neuronal survival and the effects of bFGF in explant, three dimensional and monolayer cultures of embryonic rat ventral mesencephalon *Exp. Brain Res.* **106** 275–82
- Feng X, Pelton R and Leduc M 2006 Mechanical properties of polyelectrolyte complex films based on polyvinylamine and carboxymethyl cellulose *Ind. Eng. Chem. Res.* **45** 6665–71
- Filous A, Miller J H, Coulson-Thomas Y M, Horn K P, Alilain W J and Silver J 2010 Immature astrocytes promote CNS axonal regeneration when combined with chondroitinase ABC *Dev. Neurobiology* **70** 826–41
- Ghanbarzadeh B and Almasi H 2011 Physical properties of edible emulsified films based on carboxymethyl cellulose and oleic acid *Int. J. Biol. Macromolecules* **48** 44–9
- Grealish S et al 2014 Human ESC-derived dopamine neurons show similar preclinical efficacy and potency to fetal neurons when grafted in a rat model of Parkinson's disease *Cell Stem Cell* **15** 653–65
- Harris J P, Capadona J R, Miller R H, Healy B C, Shanmuganathan K, Rowan S J, Weder C and Tyler D J 2011a Mechanically adaptive intracortical implants improve the proximity of neuronal cell bodies *J. Neural Eng.* **8** 066011
- Harris J P, Hess A E, Rowan S J, Weder C, Zorman C A, Tyler D J and Capadona J R 2011b *In vivo* deployment of mechanically adaptive nanocomposites for intracortical microelectrodes *J. Neural Eng.* **8** 046010
- Harris J P and Tyler D J 2014 Biological, mechanical, and technological considerations affecting the longevity of intracortical electrode recordings *Crit. Rev. Biomed. Eng.* **41** 435–56 (PMID: 24940658)
- He Z 2010 Intrinsic control of axon regeneration *J. Biomed. Res.* **24** 2–5
- Hopkins A M, DeSimone E, Chwalek K and Kaplan D L 2014 3D *in vitro* modeling of the central nervous system *Prog. Neurobiol.* **125** 1–25
- Huang J H, Cullen D K C-F A, Browne K D, Groff R, Zhang J, Pfister B J, Zager E L and Smith D H 2009 Long-term survival and integration of transplanted engineered nervous tissue constructs promotes peripheral nerve regeneration *Tissue Eng. A* **15** 1677–85
- Irons H R, Cullen D K, Shapiro N P, Lambert N A, Lee R H and LaPlaca M C 2008 Three-dimensional neural constructs: a novel platform for neurophysiological investigation *J. Neural Eng.* **5** 333–41
- Iwata A, Browne K D, Pfister B J, Gruner J A and Smith D H 2006 Long-term survival and outgrowth of mechanically engineered nervous tissue constructs implanted into spinal cord lesions *Tissue Eng.* **12** 101–10
- Jain A, Brady-Kalnay S M and Bellamkonda R V 2004 Modulation of Rho GTPase activity alleviates chondroitin sulfate proteoglycan-dependent inhibition of neurite extension *J. Neurosci. Res.* **77** 299–307
- Jensen W, Yoshida K and Hofmann U G 2006 *In vivo* implant mechanics of flexible, silicon-based ACREO microelectrode arrays in rat cerebral cortex *IEEE Trans. Biomed. Eng.* **53** 934–40
- Karumbaiah L, Saxena T, Carlson D, Patil K, Patkar R, Gaupp E A, Betancur M, Stanley G B, Carin L and Bellamkonda R V 2013 Relationship between intracortical electrode design and chronic recording function *Biomaterials* **34** 8061–74
- Kato-Negishi M, Morimoto Y, Onoe H and Takeuchi S 2013 Millimeter-sized neural building blocks for 3D heterogeneous neural network assembly *Adv. Healthc. Mater.* **2** 1564–70
- Kim H J 2010 Stem cell potential in Parkinson's disease and molecular factors for the generation of dopamine neurons *Biochim Biophys Acta.*
- Kozai T D, Gugel Z, Li X, Gilgunn P J, Khilwani R, Ozdoganlar O B, Fedder G K, Weber D J and Cui X T 2014 Chronic tissue response to carboxymethyl cellulose based dissolvable insertion needle for ultra-small neural probes *Biomaterials* **35** 9255–68
- Lancaster M A, Renner M, Martin C-A, Wenzel D, Bicknell L S, Hurles M E, Homfray T, Penninger J M, Jackson A P and Knoblich J A 2013 Cerebral organoids model human brain development and microcephaly *Nature* **501** 373–9
- LaPlaca M C, Vernekar V N, Shoemaker J T and Cullen D K 2010 Three-dimensional neuronal cultures *Methods in Bioengineering: 3D Tissue Engineering* ed F Berthiaume and J Morgan (Boston, MA: Artech House)
- Liu K et al 2010 PTEN deletion enhances the regenerative ability of adult corticospinal neurons *Nat. Neurosci.* **13** 1075–81
- Liu W, Ren Y, Bossert A, Wang X, Dayawansa S, Tong J, He X, Smith D H, Gelbard H A and Huang J H 2012 Allografted neurons used to repair peripheral nerve injury do not elicit overt immunogenicity *PLoS One* **7** e31675
- Mauck R L, Soltz M A, Wang C C, Wong D D, Chao P-H G, Valhmu W B, Hung C T and Ateshian G A 2000 Functional tissue engineering of articular cartilage through dynamic loading of chondrocyte-seeded agarose gels *J. Biomech. Eng.* **122** 252–60
- Mine Y, Tatarishvili J, Oki K, Monni E, Kokaia Z and Lindvall O 2013 Grafted human neural stem cells enhance several steps of endogenous neurogenesis and improve behavioral recovery after middle cerebral artery occlusion in rats *Neurobiol. Dis.* **52** 191–203
- Mingorance A, Sole M, Muneton V, Martinez A, Nieto-Sampedro M, Soriano E and del Rio J A 2006 Regeneration of lesioned entorhino-hippocampal axons *in vitro* by combined degradation of inhibitory proteoglycans and blockade of Nogo-66/NgR signaling *FASEB J.* **20** 491–3
- Moore M J et al 2006 Multiple-channel scaffolds to promote spinal cord axon regeneration *Biomaterials* **27** 419–29
- Moshayedi P, Ng G, Kwok J C, Yeo G S, Bryant C E, Fawcett J W, Franze K and Guck J 2014 The relationship between glial cell mechanosensitivity and foreign body reactions in the central nervous system *Biomaterials* **35** 3919–25
- Najafi K and Hetke J F 1990 Strength characterization of silicon microprobes in neurophysiological tissues *IEEE Trans. Biomed. Eng.* **37** 474–81
- Nguyen J K, Park D J, Skousen J L, Hess-Dunning A E, Tyler D J, Rowan S J, Weder C and Capadona J R 2014 Mechanically-compliant intracortical implants reduce the neuroinflammatory response *J. Neural Eng.* **11** 056014

- Orlacchio A, Bernardi G and Martino S 2010 Stem cells: an overview of the current status of therapies for central and peripheral nervous system diseases *Curr. Med. Chem.* **17** 595–608
- Ouardouz M and Sastry B R 2005 Activity-mediated shift in reversal potential of GABA-ergic synaptic currents in immature neurons *Brain Res. Dev. Brain Res.* **160** 78–84
- O'Connor S M, Stenger D A, Shaffer K M and Ma W 2001 Survival and neurite outgrowth of rat cortical neurons in three-dimensional agarose and collagen gel matrices *Neurosci. Lett.* **304** 189–93
- Paralikar K J, Lawrence J K and Clement R S 2006 Collagenase-aided insertion of intracortical microelectrode arrays: evaluation of insertion force and chronic recording performance *28th Annual Int. Conf. IEEE Engineering in Medicine and Biology Society, 2006 EMBS 06* pp 2958–61
- Ren H, Chen J, Wang Y, Zhang S and Zhang B 2013 Intracerebral neural stem cell transplantation improved the auditory of mice with presbycusis *Int. J. Clin. Exp. Pathol.* **6** 230–41
- Seymour J P and Kipke D R 2007 Neural probe design for reduced tissue encapsulation in CNS *Biomaterials* **28** 3594–607
- Shear D A, Tate M C, Archer D R, Hoffman S W, Hulce V D, Laplaca M C and Stein D G 2004 Neural progenitor cell transplants promote long-term functional recovery after traumatic brain injury *Brain Res.* **1026** 11–22
- Silva N A et al 2010 Development and characterization of a novel hybrid tissue engineering-based scaffold for spinal cord injury repair *Tissue Eng. A* **16** 45–54
- Silver J and Miller J H 2004 Regeneration beyond the glial scar *Nat. Rev. Neurosci.* **5** 146–56
- Sinclair S R, Fawcett J W and Dunnett S B 1999 Dopamine cells in nigral grafts differentiate prior to implantation *Eur. J. Neurosci.* **11** 4341–8
- Stabenfeldt S E, García A J and LaPlaca M C 2006 Thermoreversible laminin-functionalized hydrogel for neural tissue engineering *J. Biomed. Mater. Res. A* **77** 718–25
- Stabenfeldt S E and LaPlaca M C 2011 Variations in rigidity and ligand density influence neuronal response in methylcellulose-laminin hydrogels *Acta Biomater.* **7** 4102–8
- Stabenfeldt S E, Munglani G, García A J and LaPlaca M C 2010 Biomimetic microenvironment modulates neural stem cell survival, migration, and differentiation *Tissue Eng. A* **16** 3747–58
- Steinschneider R, Delmas P, Nedelec J, Gola M, Bernard D and Boucraut J 1996 Appearance of neurofilament subunit epitopes correlates with electrophysiological maturation in cortical embryonic neurons cocultured with mature astrocytes *Brain Res. Dev. Brain Res.* **95** 15–27
- Stichel C C, Hermanns S, Luhmann H J, Lausberg F, Niermann H, D'Urso D, Servos G, Hartwig H G and Muller H W 1999 Inhibition of collagen IV deposition promotes regeneration of injured CNS axons *Eur. J. Neurosci* **11** 632–46
- Struzyna L A, Harris J P, Katiyar K S, Chen H I and Cullen D K 2015a Restoring nervous system structure and function using tissue engineered living scaffolds. *Neural Regeneration Res.* **10** 679–85
- Struzyna L A, Wolf J A, Mietus C J, Adewole D O, Chen H I, Smith D H and Cullen D K 2015b Rebuilding brain circuitry with living micro-tissue engineered neural networks *Tissue Eng. A* **21** 2744–56
- Sudheimer K D, Winn B M, Kerndt G M, Shoaps J M, Davis K K, Fobbs Jr A J and Johnson J I 2014 *The Human Brain Atlas* (www.msu.edu/user/brains/human/index.html)
- Tang X Q, Heron P, Mashburn C and Smith G M 2007 Targeting sensory axon regeneration in adult spinal cord *J. Neurosci.* **27** 6068–78
- Tang-Schomer M D, White J D, Tien L W, Schmitt L I, Valentin T M, Graziano D J, Hopkins A M, Omenetto F G, Haydon P G and Kaplan D L 2014 Bioengineered functional brain-like cortical tissue *Proc. Natl Acad. Sci.* **111** 13811–6
- Tate C C, Shear D A, Tate M C, Archer D R, Stein D G and LaPlaca M C 2009 Laminin and fibronectin scaffolds enhance neural stem cell transplantation into the injured brain *J. Tissue Eng. Regen. Med.* **3** 208–17
- Tate M C, Garcia A J, Keselowsky B G, Schumm M A, Archer D R and LaPlaca M C 2004 Specific beta1 integrins mediate adhesion, migration, and differentiation of neural progenitors derived from the embryonic striatum *Mol. Cell. Neurosci* **27** 22–31
- Tate M C, Shear D A, Hoffman S W, Stein D G, Archer D R and LaPlaca M C 2002 Fibronectin promotes survival and migration of primary neural stem cells transplanted into the traumatically injured mouse brain *Cell. Transplantation* **11** 283–95
- Tate M C, Shear D A, Hoffman S W, Stein D G and LaPlaca M C 2001 Biocompatibility of methylcellulose-based constructs designed for intracerebral gelation following experimental traumatic brain injury *Biomaterials* **22** 1113–23
- Tsai E C, Dalton P D, Shoichet M S and Tator C H 2004 Synthetic hydrogel guidance channels facilitate regeneration of adult rat brainstem motor axons after complete spinal cord transection *J. Neurotrauma* **21** 789–804
- Tsai P S, Kaufhold J P, Blinder P, Friedman B, Drew P J, Karten H J, Lyden P D and Kleinfeld D 2009 Correlations of neuronal and microvascular densities in murine cortex revealed by direct counting and colocalization of nuclei and vessels *J. Neurosci.* **29** 14553–70
- Turner J, Shain W, Szarowski D, Andersen M, Martins S, Isaacson M and Craighead H 1999 Cerebral astrocyte response to micromachined silicon implants *Exp. Neurology* **156** 33–49
- Vukasinovic J, Cullen D K, LaPlaca M and Glezer A 2009 A microperfused incubator for tissue mimetic 3D cultures *Biomed. Microdevices* **11** 1155–65
- Wagenaar D A, Pine J and Potter S M 2006 An extremely rich repertoire of bursting patterns during the development of cortical cultures *BMC Neurosci.* **7** 11
- Warnock F V and Benham P P 1965 *Mechanics of Solids and Strength of Materials* (Boston, MA: Pitman)
- Yip P K, Wong L F, Sears T A, Yanez-Munoz R J and McMahon S B 2010 Cortical overexpression of neuronal calcium sensor-1 induces functional plasticity in spinal cord following unilateral pyramidal tract injury in rat *PLoS Biol.* **8** e1000399
- Yoo S J, Kim J, Lee C S and Nam Y 2011 Simple and novel three dimensional neuronal cell culture using a micro mesh scaffold *Exp Neurobiol.* **20** 110–5